SUPPORTING INFORMATION

From nonconductive MOF to proton-conducting metal-HOFs: a new class of reversible transformations induced by solvent-free mechanochemistry

Magdalena Lupa-Myszkowska,[a,b] Marcin Oszajca,[a] and Dariusz Matoga*[a]

[a]Faculty of Chemistry, Jagiellonian University, Gronostajowa 2, 30-387 Kraków, Corresponding author: dariusz.matoga@uj.edu.pl

[b]Doctoral School of Exact and Natural Sciences, Jagiellonian University, ul. prof. S. Łojasiewicza 11, 30-348 Kraków

Contents:

Synthetic procedures and control experiments

All chemicals and solvents (of analytical grade) were purchased from commercial sources (Merck, TCI, Avantor, Polmos) and were used without further purification. Ethanol (Polmos) contained water (8% by volume).

Synthesis of JUK-1

JUK-1 was synthesized according to a method described in literature.[1] IR (ATR, cm^{-1}): v(C-O) 1398vs, $v(COO_s)$ 1415m, $v(C=C_{ar})$ 1550s, $v(COO_{as})$ 1600vs, v(C=O) 1645m, $v(CH_{ethanol})$ 2972w, v(OH) 3270m

Synthesis of JUK-2

JUK-2 was synthesized according to a method described in literature.[2] IR (ATR, cm^{-1}): IR (ATR, cm^{-1}): v(C-O) 1406vs, $v(COO_s)$ 1413s, $v(C=C_{ar})$ 1544s, $v(COO_{as})$ 1576vs, v(C=O) 1671m, $v(CN)_{SCN}$ 2102vs, v(OH) 3189m

Synthesis of Mn-HOF-MA - $\{(CH_3NH_3)_2[Mn(ina)_2(NCS)_2(H_2O)_2]\cdot xH_2O\}_n$

JUK-1 (100.0 mg, 0.138 mmol) and CH_3NH_3SCN (49.6 mg, 0.550 mmol) were ground in an agate mortar in air at room temperature for approx. 10 min. with addition 75 µL 92% EtOH (LAG, liquid-assisted grinding; 1:2 metal/thiocyanate ratio). Elem. anal.: Calc. for $C_{16}H_{24}MnN_6O_6S_2$ ($\{(CH_3NH_3)_2[Mn(ina)_2(NCS)_2(H_2O)_2]\}_n$): C 37.28, H 4.69, N 16.30, S 12.44%. Found: C 36.84, H 4.69, N 16.44, S 12.11%. IR (ATR, cm^{-1}): $v(COO_s)$ 1372s, $v(COO_s)$ 1413m, $v(C=C_{ar})$ 1549s, $v(COO_{as})$ 1581m, $v(COO_{as})$ 1636s, $v(CN)_{SCN}$ 2078vs, $v(NH)_{methylammonium}$ 3049m.

Synthesis of Mn-HOF-FA - $\{(CH(NH_2)_2)_2[Mn(ina)_2(NCS)_2(H_2O)_2]\cdot xH_2O\}_n$

JUK-1 (100.0 mg, 0.138 mmol) and $CH(NH_2)_2SCN$ (56.8 mg, 0.550 mmol) were ground in an agate mortar in air at room temperature for approx. 10 min. with addition 75 µL 92% EtOH (LAG, liquid-assisted grinding; 1:2 metal/thiocyanate ratio). Elem. anal.: Calc. for $C_{16}H_{22}MnN_8O_6S_2$ ($\{(CH(NH_2)_2)_2[Mn(ina)_2(NCS)_2(H_2O)_2]\}_n$): C 35.49, H 4.10, N 20.69, S 11.84%. Found: C 34.79, H 4.17, N 21.40, S 12.61%. IR (ATR, cm^{-1}): $v(COO_s)$ 1392s, $v(COO_s)$ 1416w, $v(C=C_{ar})$ 1538s, $v(COO_{as})$ 1583m, $v(COO_{as})$ 1651m, $v(CN)_{formamidine}$ 1721vs, $v(CN)_{SCN}$ 2098vs, $v(NH)_{formamidine}$ 3051m.

Control experiments to test the possibility of formation of Mn-HOF-MA and Mn-HOF-FA in solution

a) Several trials described below have been carried out for saturated alcohol solutions of CH_3NH_3SCN and $CH(NH_2)_2SCN$. In all experiments JUK-1 (30 mg) and salts were mixed in an ethanol (2.0 mL) and left for approx. 48h at room temperature.
   In all the trials Mn-HOF-MA and Mn-HOF-FA were not formed. All solid samples have been screened with IR (Figure S10).

b) An appropriate amount of thiocyanate salts (CH_3NH_3SCN – 90.14 mg, 1.0 mmol and $CH(NH_2)_2SCN$ 103,14 mg, 1.0 mmol) was added to the standard synthesis of JUK-1. It was left for 2 weeks at room temperature after which the IR and PXRD (Figures S11 and S12 below) of the solid samples were measured – the *de novo* synthesis test.

Reversibility of Mn-HOF-MA and Mn-HOF-FA formation

In all experiments Mn-HOF-MA (30 mg) and Mn-HOF-FA (30 mg) were immersed in ethanol (5.0 mL) for approx. 1 h at room temperature. During this time ethanol was changed 6 times. All solid samples have been screened with PXRD (Figure SX below).

Samples preparation for EIS measurements

Prior to a series of EIS measurements at a given relative humidity (RH), approx. 30 mg of the material was equilibrated in a humidity chamber for 1 day at a specified RH (75 - 30%) at 25^{o}C. For anhydrous measurement approx. 30 mg of the material was equilibrated in a vacuum dryer for 1 day at 100^{o}C.

Details of physical measurements

Carbon, hydrogen and nitrogen were determined using an Elementar Vario MICRO Cube elemental analyzer.

Thermogravimetric analyses (TGA) were performed on a Mettler-Toledo TGA/SDTA 851^{e} instrument with a heating rate of 10°C min^{-1} in a temperature range of 25 – 600°C (approx. sample weight of 10 mg). The measurements were performed at atmospheric pressure under argon flow.

FTIR spectra were recorded on a Thermo Scientific Nicolet iS10 FT-IR spectrophotometer equipped with an iD7 diamond ATR attachment.

Powder X-ray diffraction (PXRD) patterns were recorded at room temperature (295 K) on a Rigaku Miniflex 600 diffractometer with Cu-Kα radiation (λ = 1.5418 Å) in a 2θ range from 3° to 45° with a 0.02° step and 3° min^{-1} scan speed.

Water (293 K) adsorption/desorption studies were performed on an Autosorb iQ-CXR-XR EPDM volumetric analyzer (Quantachrome Instruments). Prior to the physisorption measurements, JUK-1 sample was activated at 100°C under vacuum for 8h. JUK-2 and Mn-HOFs samples were activated at 25°C under vacuum for 24h. The second and third cycle of

water vapor measurement were performed without any further thermal activations for JUK-2 and Mn-HOFs samples, except the initial one. In the case of JUK-1 sample, additional activation was needed after each cycle (100°C under vacuum for 8h).

Electrochemical Impedance Spectroscopy (EIS) measurements were performed using Hioki IM3570 impedance analyzer on pre-conditioned samples (see Samples preparation for EIS Measurement above) pressed between two platinum electrodes (8 mm diameter) in a PTFE tube of a Fine Instruments PIP- 260 probe (Elektronika Jądrowa Kraków, Poland), and kept in KK 115 TOP+ climatic chamber with an ultrasonic humidifier and a temperature control (the measurements with humidity control) or in a vacuum dryer Memmert, VO 200 (the measurements at the temperatures above 100°C). The measurements were carried out in a quasi-four-probe setup in a frequency range from 4 Hz to 5 MHz, potential of 100 mV, alternating current and temperature range from 25 to 60°C (for the measurements in 30 – 75% RH) or for 100°C (for the anhydrous measurements), and with pre-measurement sample conditioning for 1 h at each temperature. The proton conductivity (σ, S cm^{-1}) of each sample was estimated by using the equation:

$$\sigma = L/(RA)$$

where L (cm) is the sample thickness and A (cm^2) is the cross-sectional area of the measured pellet; R (Ω) is the resistance as the real part of the measured impedance.

The morphology and chemical composition of studied materials were analysed using scanning electron microscopy (Helios 5 Hydra DualBeam, Thermo Fisher Scientific, USA) equipped with energy-dispersive X-ray spectroscopy (EDS, Gatan, USA). The EDS maps of elemental composition were prepared under 200 000 x magnification. The samples were deposited on a silicon substrate. For imaging, the samples were additionally sputtered with gold.

PXRD data collection and structure refinement details

The powder diffraction data used in the structure solution was collected on a PANalytical X'Pert PRO MPD with a copper source operating at 40 kV and 30 mA in Debye-Scherrer geometry using a focusing mirror and a PIXCEL position sensitive detector. The measurements used samples packed inside a 0.5 mm diameter borosilicate glass capillaries and the data was registered over a 4-90^o 2-theta range with measurement time of 21 h and 40 min and 20 h for Mn-HOF-MA and Mn-HOF-FA respectively. The datasets were indexed, analysed regarding compatible space groups and structure solution attempts with direct methods were undertaken using EXPO2014[3]. Additional work with obtaining a working model of the structure was done using FOX[4]. The obtained models seemed convincing and managed to be refined using Rietveld refinement as implemented in Jana2020[5]. The relatively complicated models required using rigid body description for the aromatic rings of the isonicotinate ligands. Additionally, the water molecules located in both structures did

not have assigned positions for hydrogen atoms due to the fact that locating those atoms from differential electron density maps was impossible. To address the missing electrons in both structures oxygen atoms were assigned with increased occupancies (1.25).

Table S1. Data collection and structure refinement details.

Compound name	**Mn-HOF-MA**	**Mn-HOF-FA**
CCDC deposition numbers	2288812	2288811
Chemical formula	$C_{16}H_{24}MnN_6O_6S_2$	$C_{16}H_{22}MnN_8O_6S_2$
Formula Mass	515.47	541.46
Crystal data		
Crystal system, space group	Monoclinic, $P2_1/c$	Monoclinic, An
Temperature (K)	293	293
a, *b*, *c* (Å)	10.4862, 15.4994, 7.56251	14.3651, 14.91024, 13.24655
α, β, γ (°)	90, 98.534, 90	90, 117.406, 90
Unit cell volume/Å^3	1215.52	2518,81
Z	2	4
Experimental details		
Radiation type	Cu Kα	Cu Kα
Absorption coefficient, μ/mm^{-1}	6.391	6.225
R_{int}	0.0771	0.0656
2θ range/step/°	4.017 – 89.986/0.013	4.007 – 89.995/0.013
Refinement details		
No. of parameters/restrains	73/17	104/52
Final R_1 value ($I > 2\sigma(I)$)	0.1137	0.0806
Final $wR(F^2)$ values ($I > 2\sigma(I)$)	0.0767	0.0545
Final R_p / R_{wp}	0.0209/0.0291	0.0203/0.0268
Goodness of fit	1.6856	1.5113

Figures and Tables

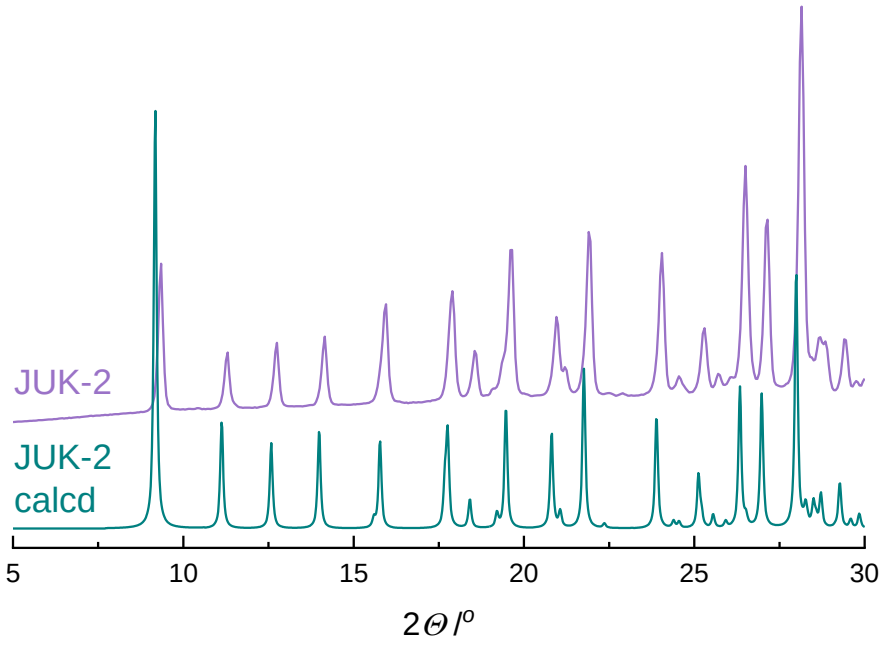

Figure S1. PXRD patterns JUK-2 calculated from SC-XRD data (green) and the as-synthesized bulk material (purple).

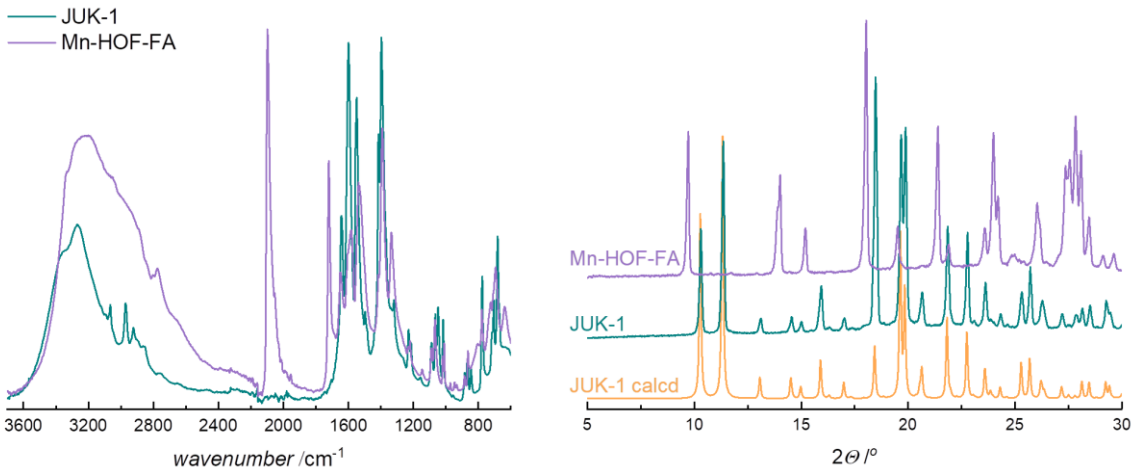

Figure S2. IR spectra (left): JUK-1 as-synthesized (green) and Mn-HOF-FA (JUK-1 after LAG with CH(NH2)2SCN (FA) at 1:2 molar ratio (purple). PXRD patterns (right): JUK-1 calculated from SC-XRD data (yellow), the as-synthesized bulk material (green), and Mn-HOF-FA (purple).

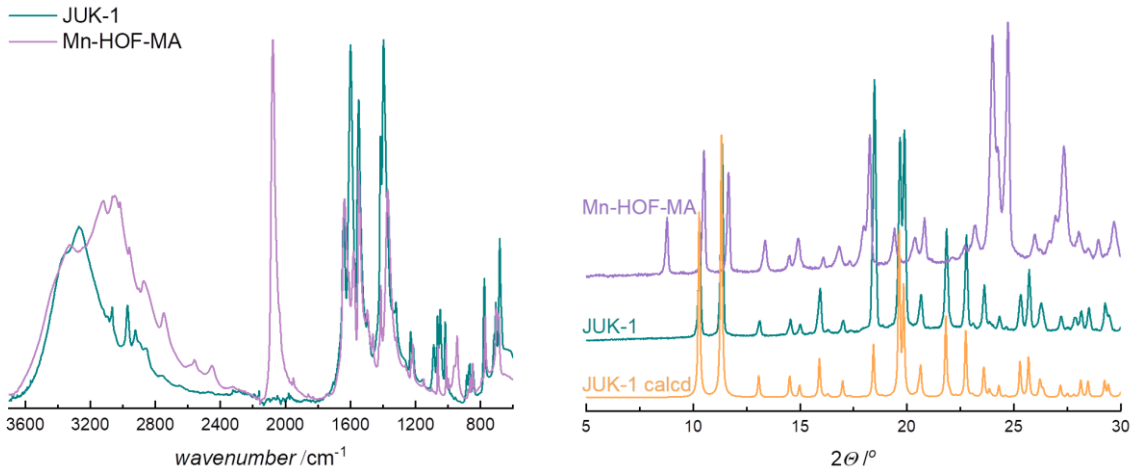

Figure S3. IR spectra (left): JUK-1 as-synthesized (green) and Mn-HOF-MA (JUK-1 after LAG with CH_3NH_3SCN (MA) at 1:2 molar ratio (purple). PXRD patterns (right): JUK-1 calculated from SC-XRD data (yellow), the as-synthesized bulk material (green), and Mn-HOF-MA (purple).

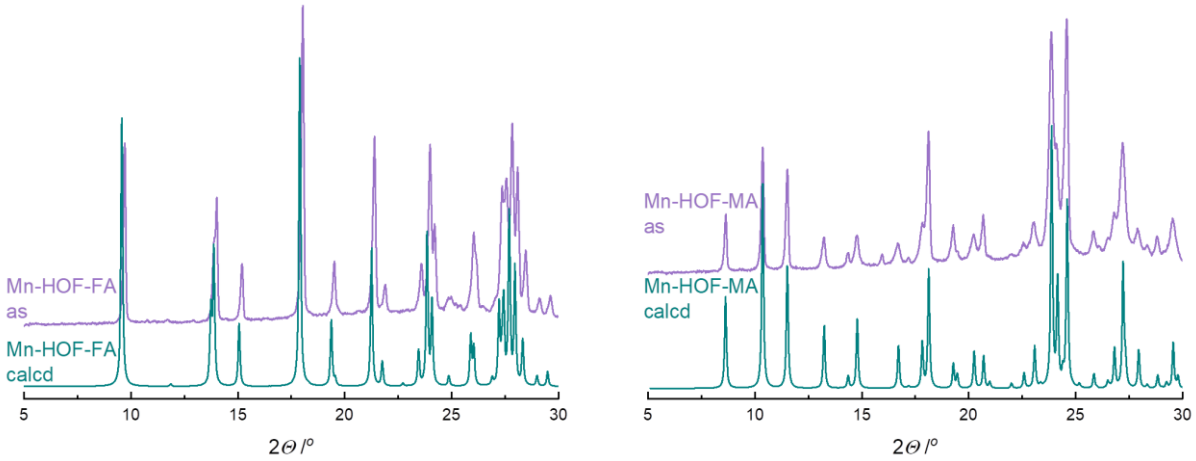

Figure S4. PXRD patterns Mn-HOF-FA (left) and Mn-HOF-MA (right) calculated from PXRD data (green) and the as-synthesized bulk material (purple).

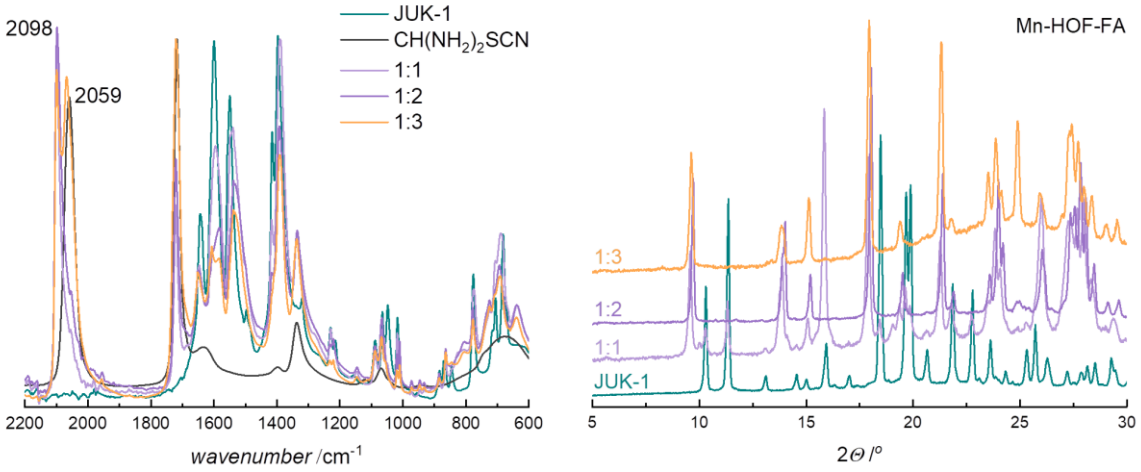

Figure S5. IR spectra (left) and PXRD patterns (right) of mixtures after grinding JUK-1 (green) with various amounts of $CH(NH_2)_2SCN$; 1:1, 1:2, 1:3 (given as JUK-1 to $CH(NH_2)_2SCN$ ratio).

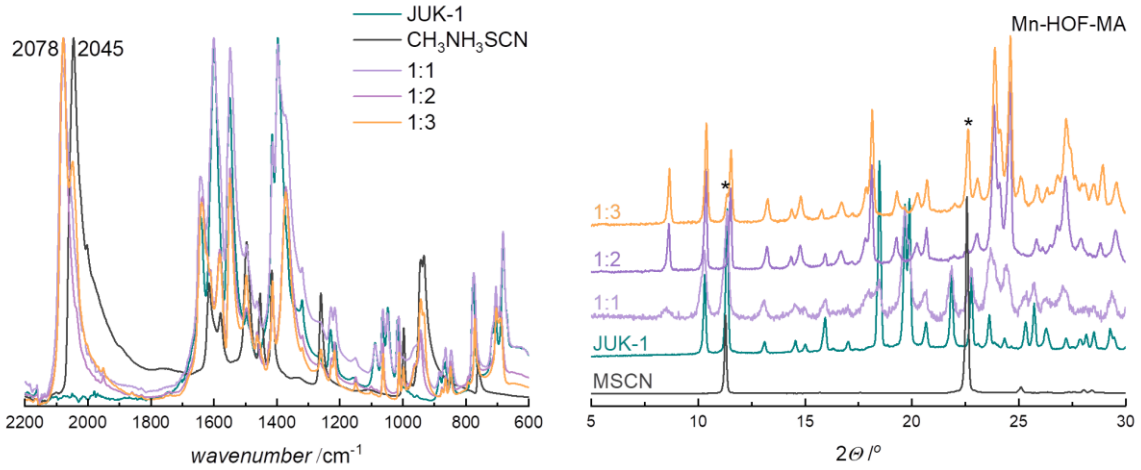

Figure S6. IR spectra (left) and PXRD patterns (right) of mixtures after grinding JUK-1 (green) with various amounts of CH_3NH_3SCN; 1:1, 1:2, 1:3 (given as JUK-1 to CH_3NH_3SCN ratio).

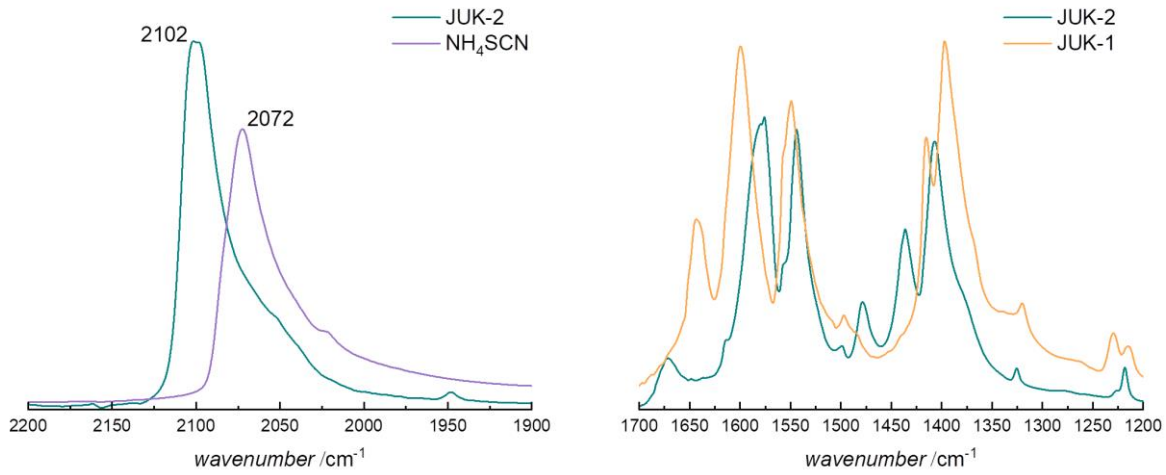

Figure S7. IR spectra for JUK-2 (green) and NH_4SCN (purple) showing ν(CN) range (left) and for JUK-2 (green) and JUK-1 (yellow) showing carboxylate range (right).

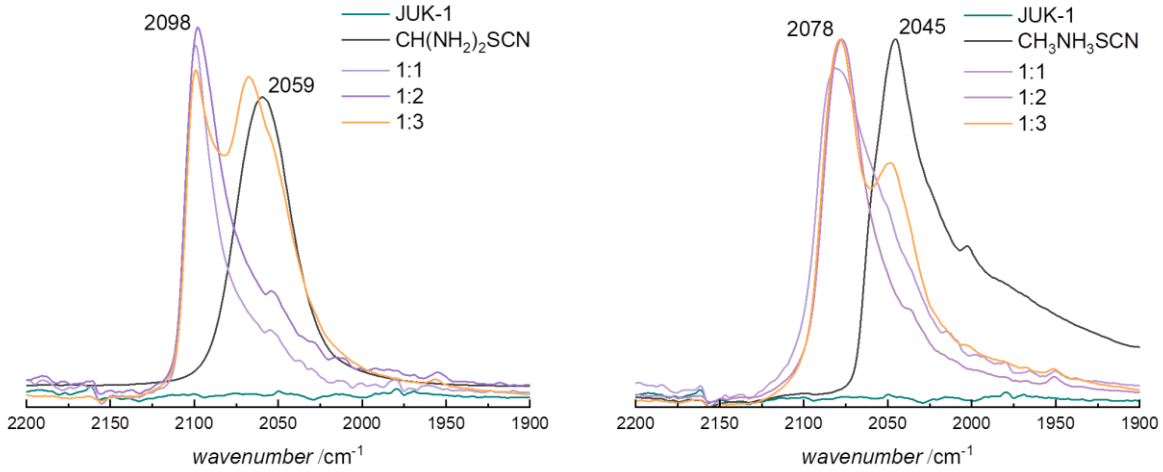

Figure S8. IR spectra of mixtures after grinding JUK-1 (green) with various amounts of $CH(NH_2)_2SCN$ or CH_3NH_3SCN; 1:1, 1:2, 1:3, (given as the JUK-1 to CH(NH2)2SCN or CH_3NH_3SCN ratio) showing ν(CN) range.

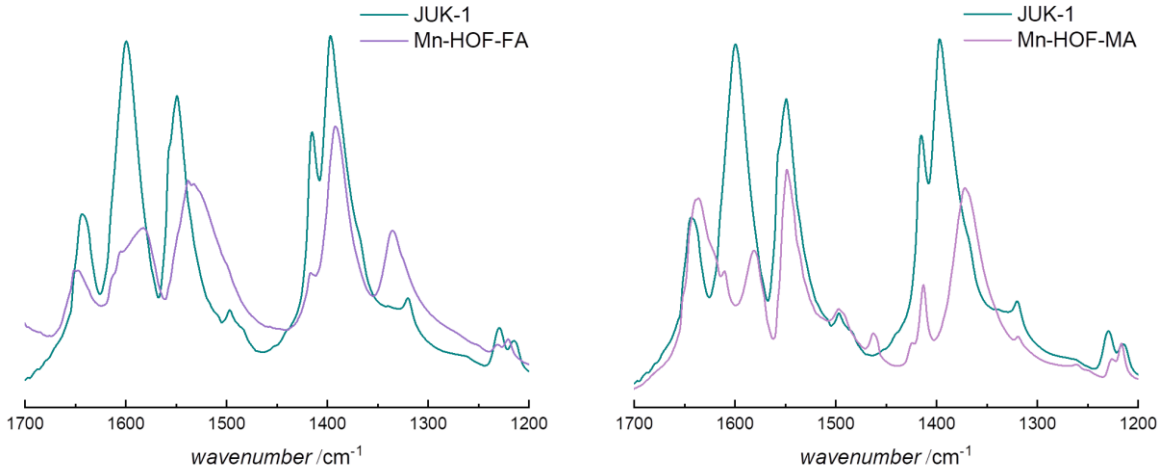

Figure S9. IR spectra for JUK-1 (green) and Mn-HOFs (purple) showing carboxylate range.

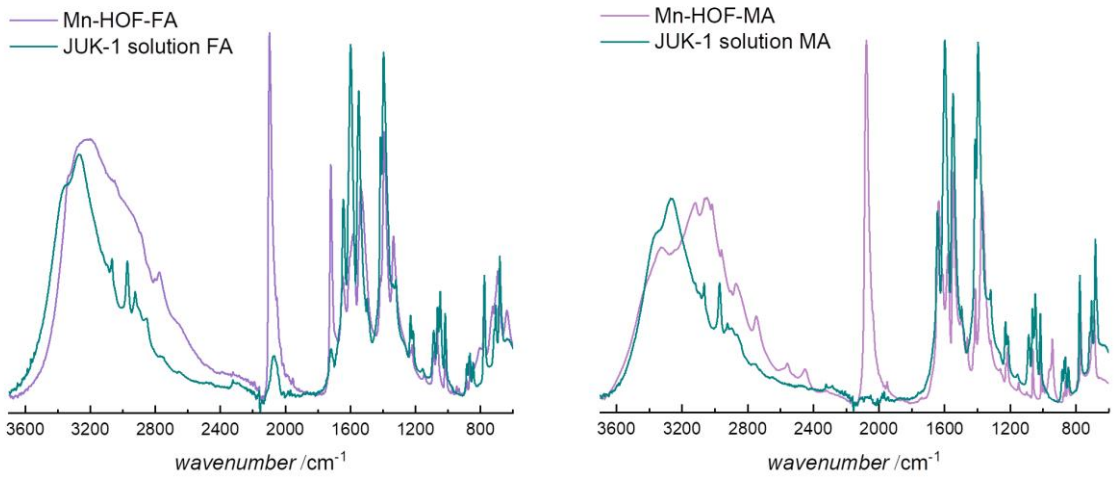

Figure S10. IR spectra of the as-synthesized JUK-1 (green) immersed in saturated solutions of $CH(NH_2)_2SCN$ (FA) or CH_3NH_3SCN (MA) in ethanol. The IR spectra of Mn-HOFs (purple) are given for comparison.

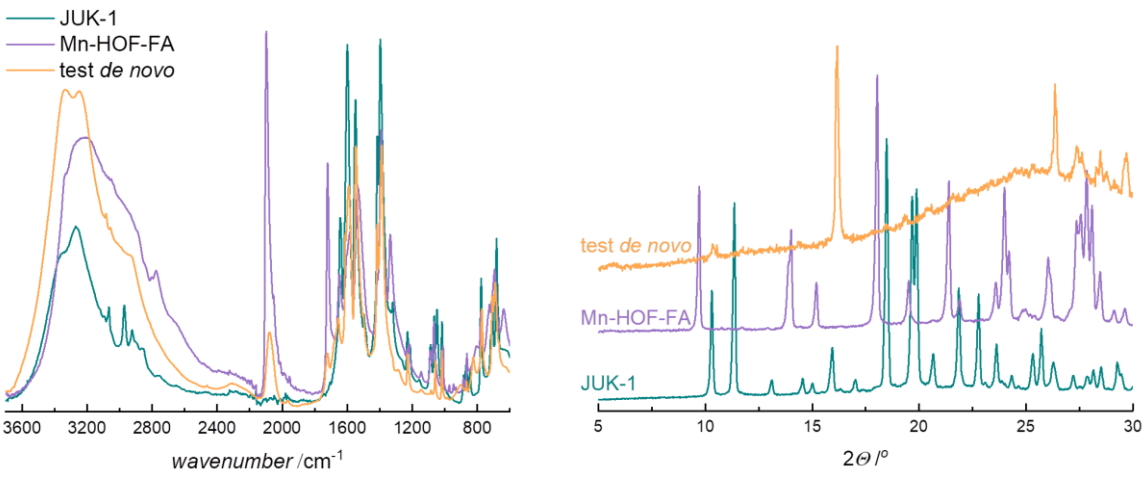

Figure S11. IR spectra (left) and PXRD pattern (right) for solid sample from the *de novo* synthesis test for Mn-HOF-FA. The IR spectra of Mn-HOF-FA (purple) and JUK-1 (green) are given for comparison.

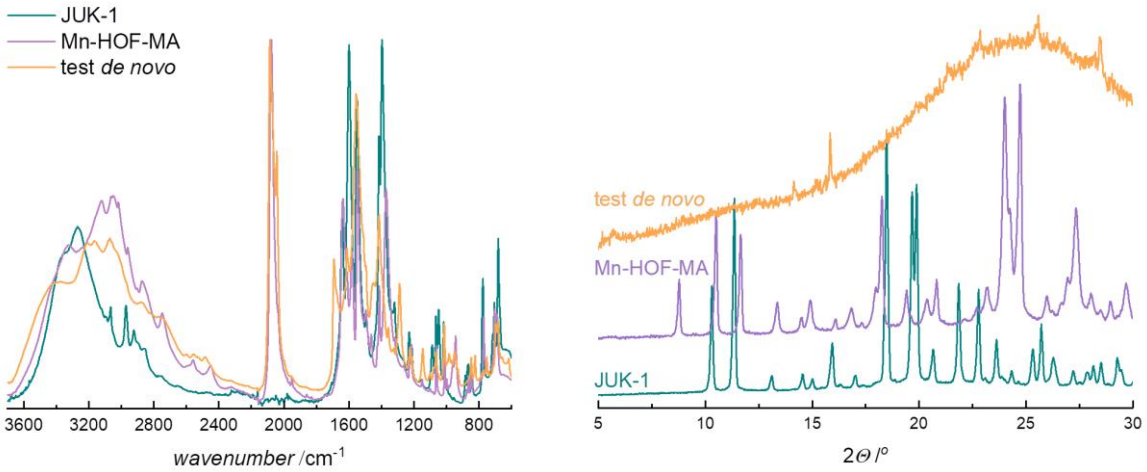

Figure S12. IR spectra (left) and PXRD pattern (right) for solid sample from the *de novo* synthesis test for Mn-HOF-MA. The IR spectra of Mn-HOF-MA (purple) and JUK-1 (green) are given for comparison.

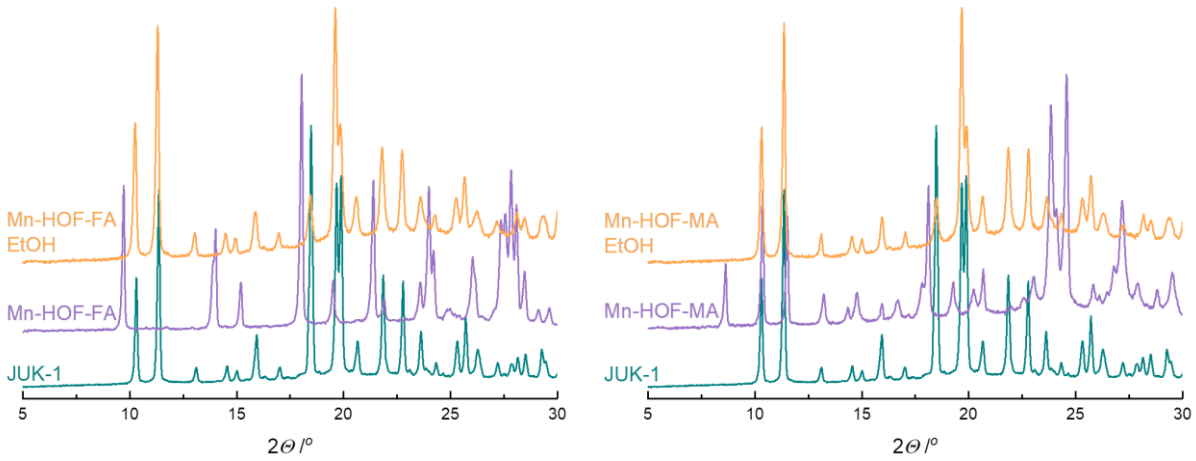

Figure S13. Reversibility of Mn-HOFs formation. PXRD patterns: JUK-1 as-synthesized (green), Mn-HOFs (purple) and Mn-HOFs immersed in ethanol at room temperature for 1 h – Mn-HOFs EtOH (yellow). $CH(NH_2)_2SCN$ - "FA", CH_3NH_3SCN - "MA".

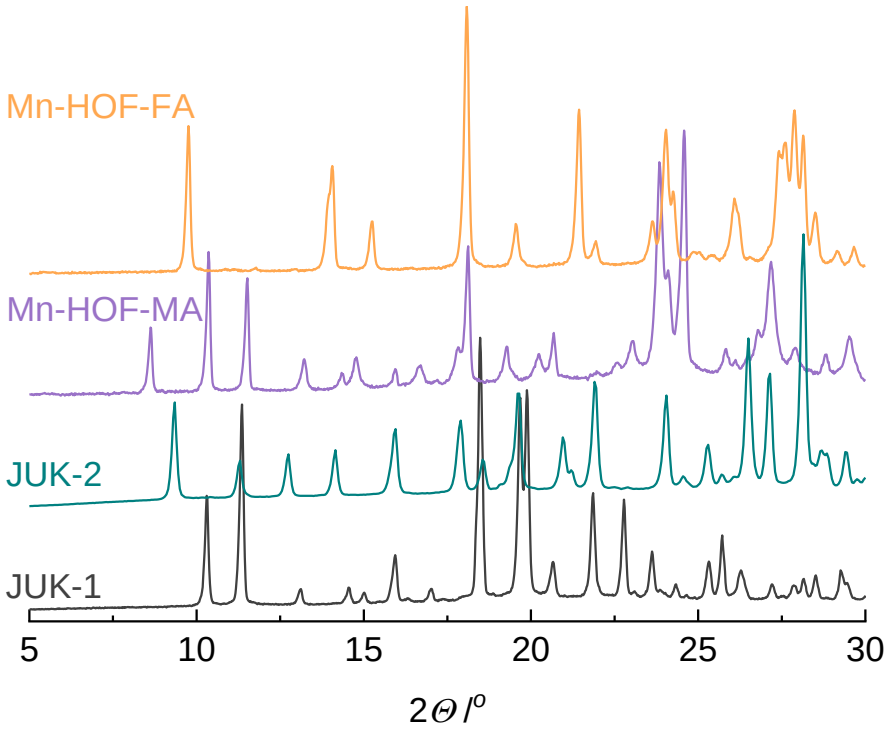

Figure S14. PXRD patterns: JUK-1 as-synthesized (black), JUK-2 (green) - JUK-1 after LAG with NH_4SCN, Mn-HOF-MA (purple) - JUK-1 after LAG with CH_3NH_3SCN and Mn-HOF-FA (yellow) - JUK-1 after LAG with $CH(NH_2)_2SCN$. All at 1:2 metal/thiocyanate ratio.

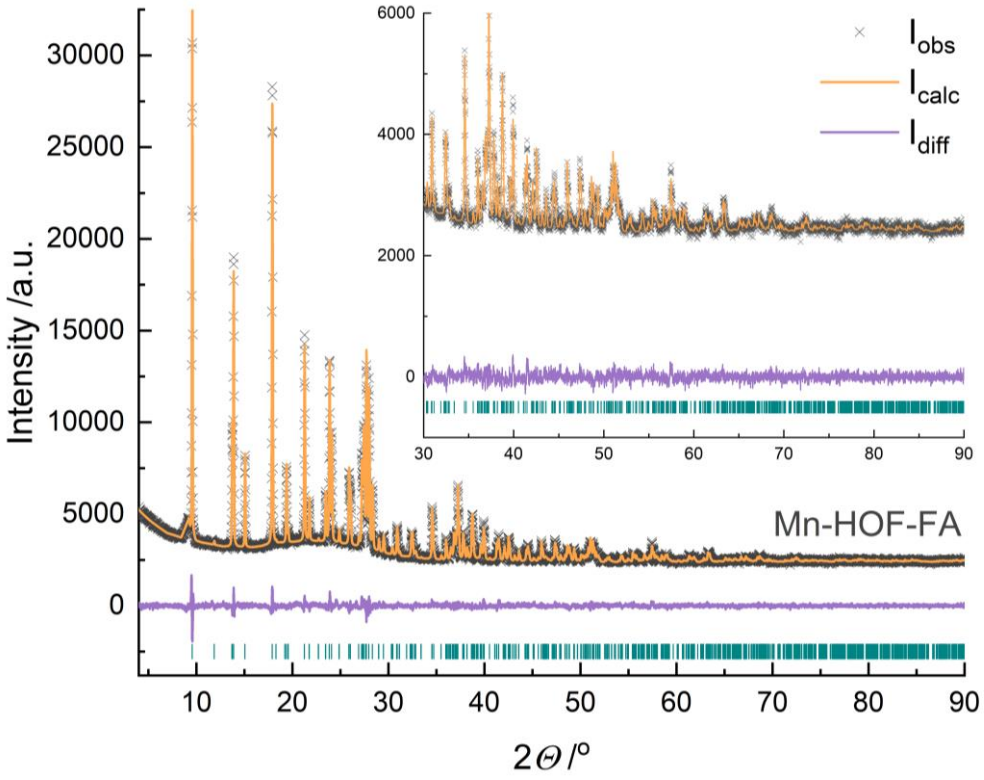

Figure S15. The observed (black cross) and calculated (yellow line) PXRD patterns of Mn-HOF-FA along with the difference curve (bottom purple line).

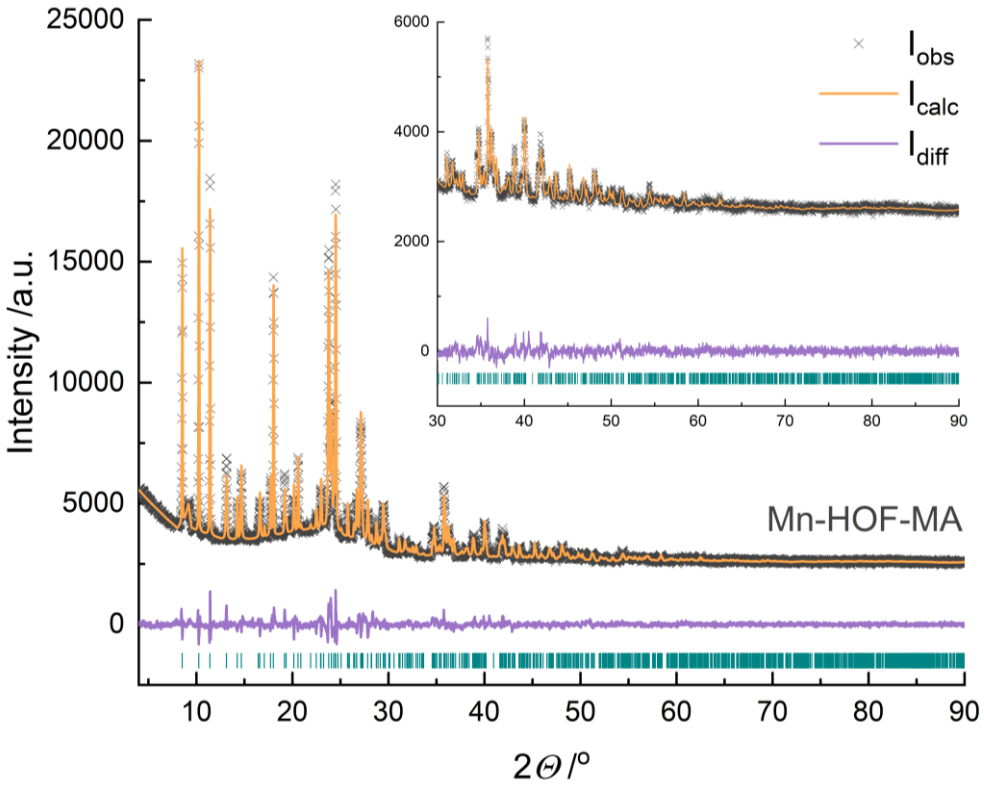

Figure S16. The observed (black cross) and calculated (yellow line) PXRD patterns of Mn-HOF-MA along with the difference curve (bottom purple line).

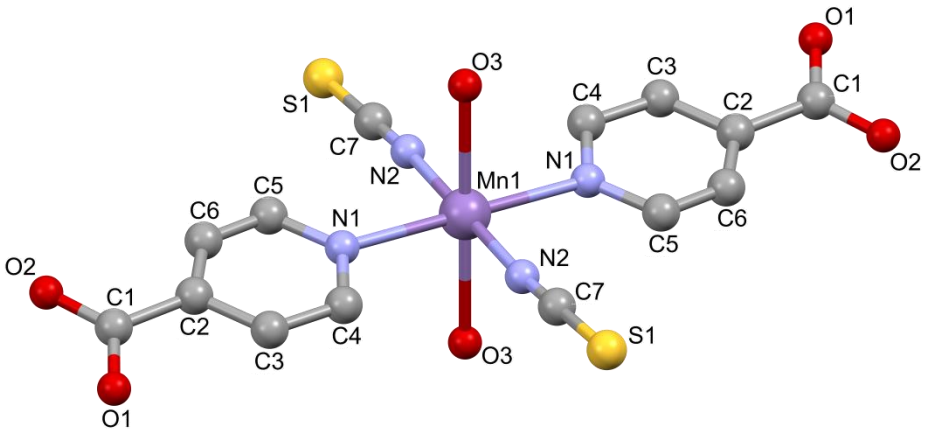

Figure S17. Partial view of the X-ray crystal structure of the anionic framework in Mn-HOF-MA with atom labeling scheme.

Table S2. Selected bond lengths for Mn-HOF-MA.

Type	Atom code	Length [Å]
Mn-X	Mn1-N1	2.349
	Mn1-N2	2.028
	Mn1-O3	2.336

S-C	S1-C7	1.646
C-N	C7-N2	1.147
C-O (carboxylate)	C1-O1	1.252
	C1-O2	1.252

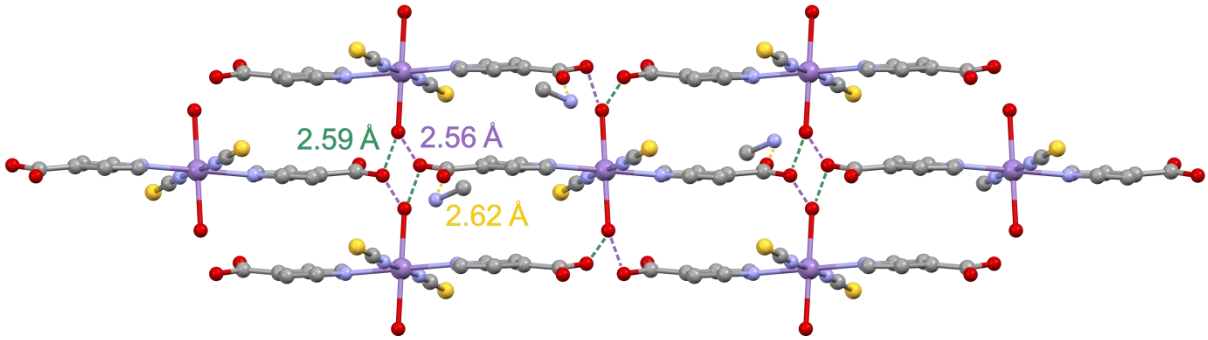

Figure S18. Framework-stabilizing O–H···O hydrogen bonds, shown as dashed lines in Mn-HOF-MA viewed along the a axis (H atoms omitted, Mn – purple, O – red, N – blue, S – yellow, C – grey). Appropriate colour of the numbers corresponds to the length of the hydrogen bond in the same colour as the line.

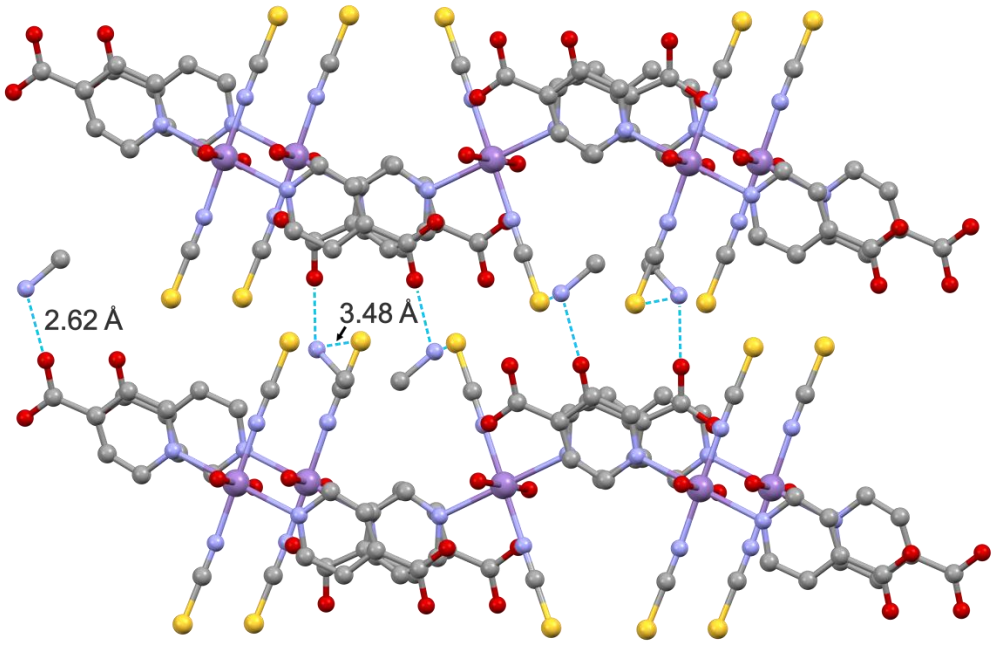

Figure S19. Interlayer N–H···O and N–H···S hydrogen bonds, shown as blue lines in Mn-HOF-MA (H atoms omitted, Mn – purple, O – red, N – blue, S – yellow, C – grey).

Table S3. Comparison of lengths of hydrogen bonds present in the Mn-HOF-MA.

Type	Atom code	Length [Å]
O-H···O	O3····O2	2.556
	O3····O2	2.593
N-H···O	N3····O1	2.619
N-H···S	N1····S3	3.481

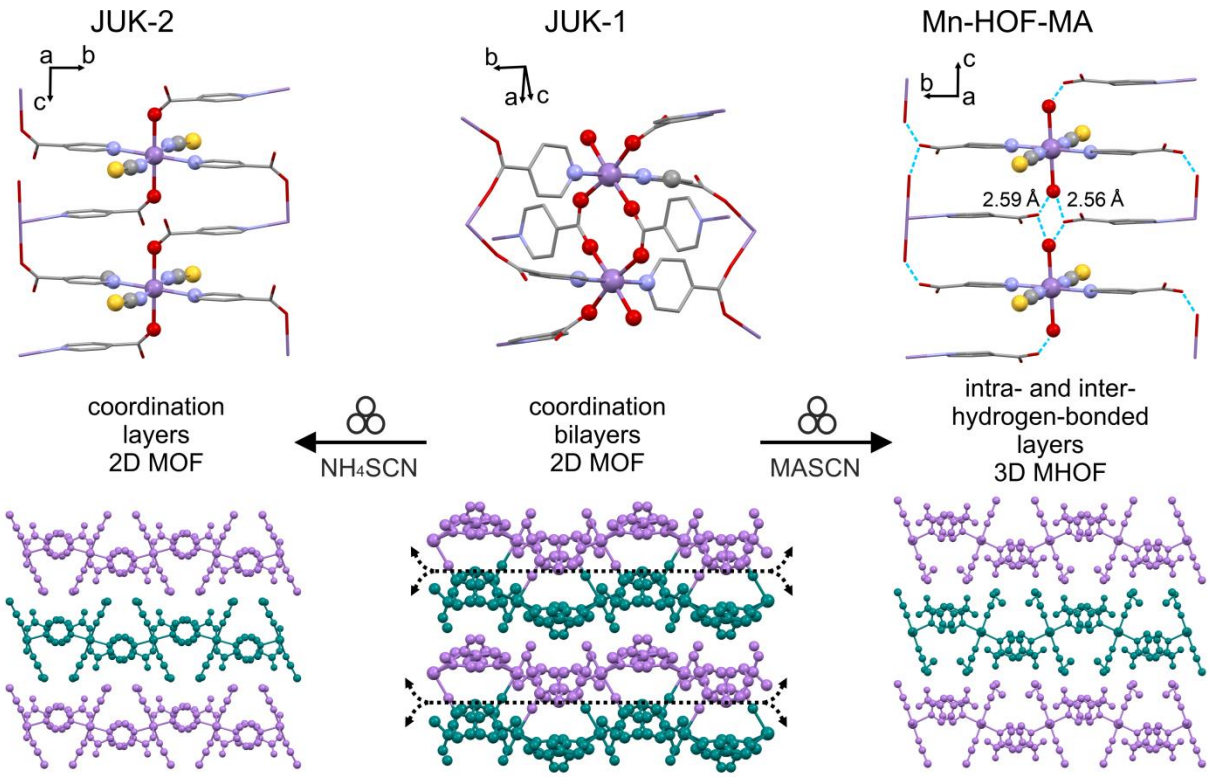

Figure S20. Structural transformation between JUK-1 and Mn-HOF-MA or JUK-2. Structural details of molecular rearrangement inside the coordination region (H atoms omitted, Mn – purple, O – red, N – blue, S – yellow, C – grey) – top. Stacked bilayers in JUK-1 and layers in JUK-2 and Mn-HOF-MA viewed along the c axis (cations omitted for clarity) – bottom.

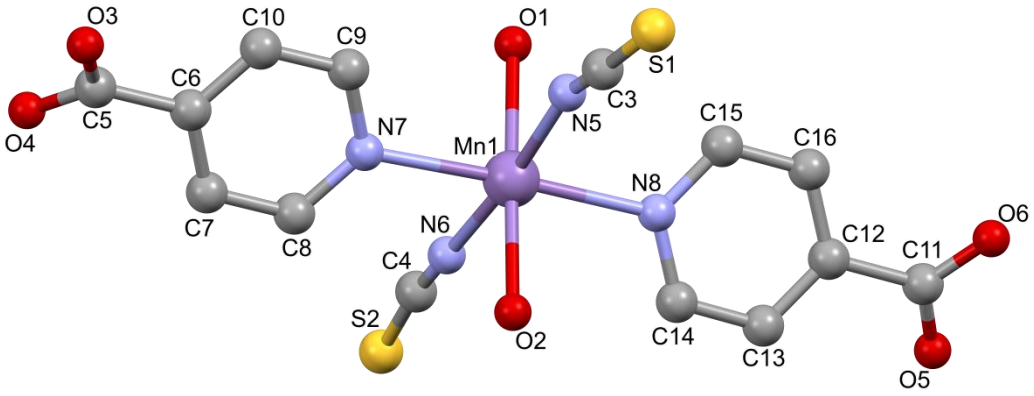

Figure S21. Partial view of the X-ray crystal structure of the anionic framework in Mn-HOF-FA with atom labeling scheme.

Table S4. Selected bond lengths for Mn-HOF-FA.

Type	Atom code	Length [Å]
Mn-X	Mn1-N5	2.237
	Mn1-N6	2.195
	Mn1-N7	2.316
	Mn1-N8	2.297
	Mn1-O1	2.252

	Mn1-O2	2.201
S-C	S1-C3	1.635
	S2-C4	1.644
C-N	C3-N5	1.160
	C4-N6	1.166
C-O (carboxylate)	C5-O3	1.251
	C5-O4	1.246
	C11-O5	1.247
	C11-O6	1.250

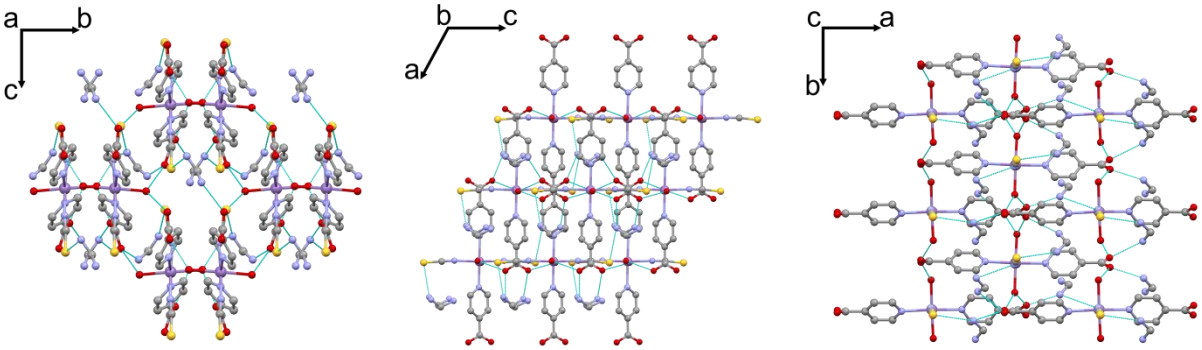

Figure S22. Framework-stabilizing hydrogen bonds, shown as dashed lines in Mn-HOF-FA viewed along all axis (H atoms omitted, Mn – purple, O – red, N – blue, S – yellow, C – grey).

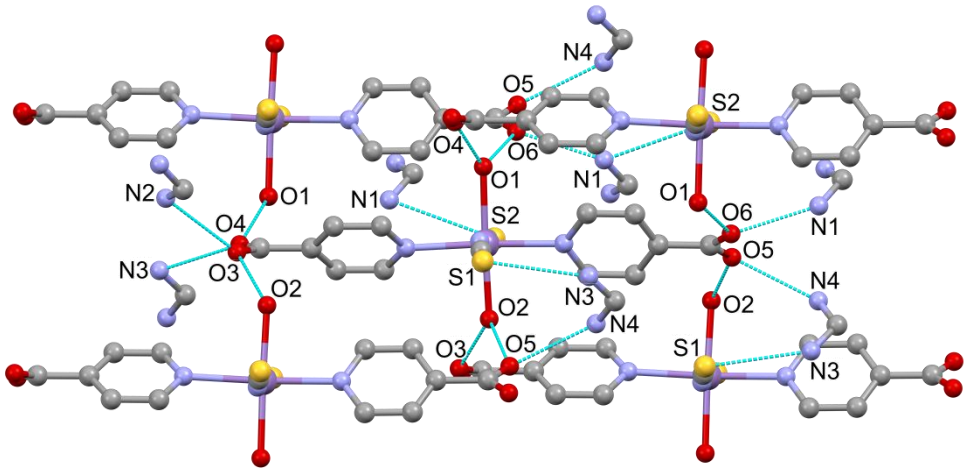

Figure S23. Framework-stabilizing hydrogen bonds, shown as dashed lines in Mn-HOF-FA viewed along the c axis with atom labeling scheme (H atoms omitted, Mn – purple, O – red, N – blue, S – yellow, C – grey).

Table S5. Comparison of lengths of hydrogen bonds present in the Mn-HOF-FA.

Type	Atom code	Length [Å]
O-H···O	O1····O4	2.542
	O2····O3	2.784
	O1····O6	2.796
	O2····O5	2.847
N-H···O	N3····O4	2.686
	N1····O6	2.688

	N4····O5	2.862
	N2····O3	2.896
N-H···S	N3····S1	3.157
	N1····S2	3.341

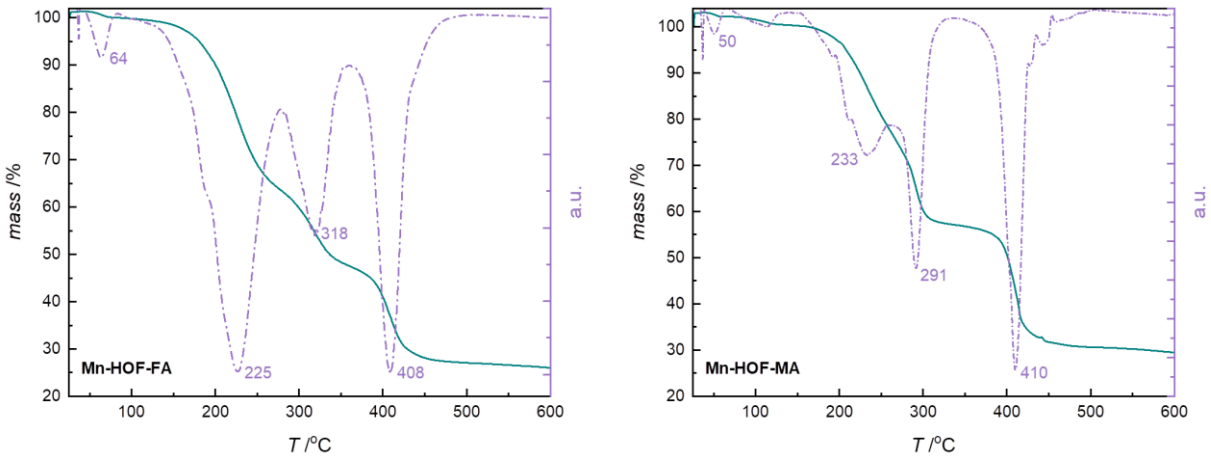

Figure S24. TG (green) and dTG (purple) curves for Mn-HOF-FA (left) and Mn-HOF-MA (right) showing stepwise weight loss upon heating.

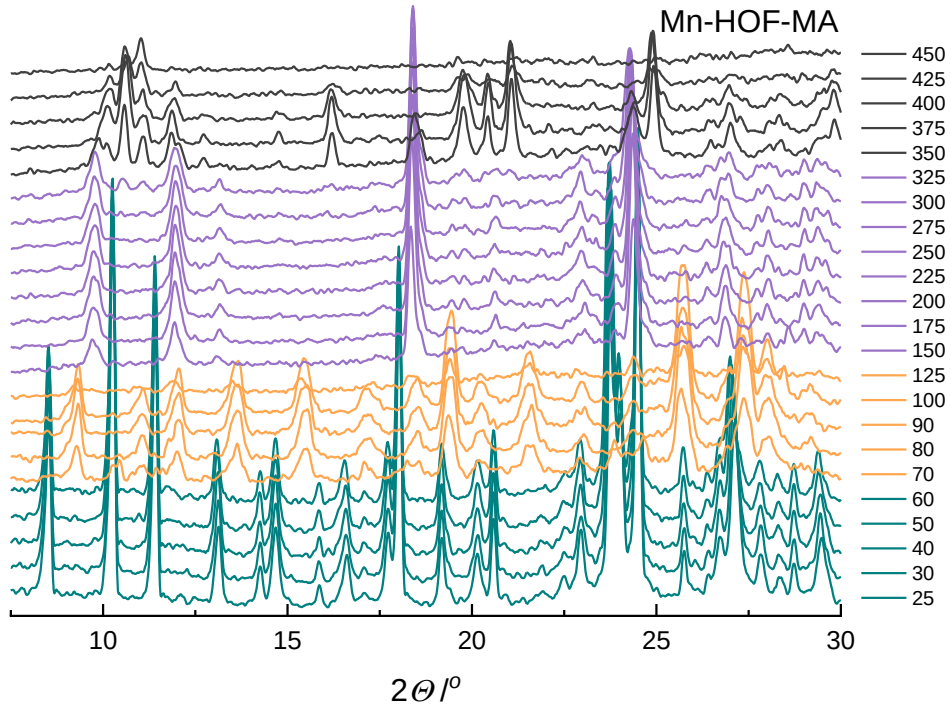

Figure S25. Temperature-dependent PXRD patterns for Mn-HOF-MA.

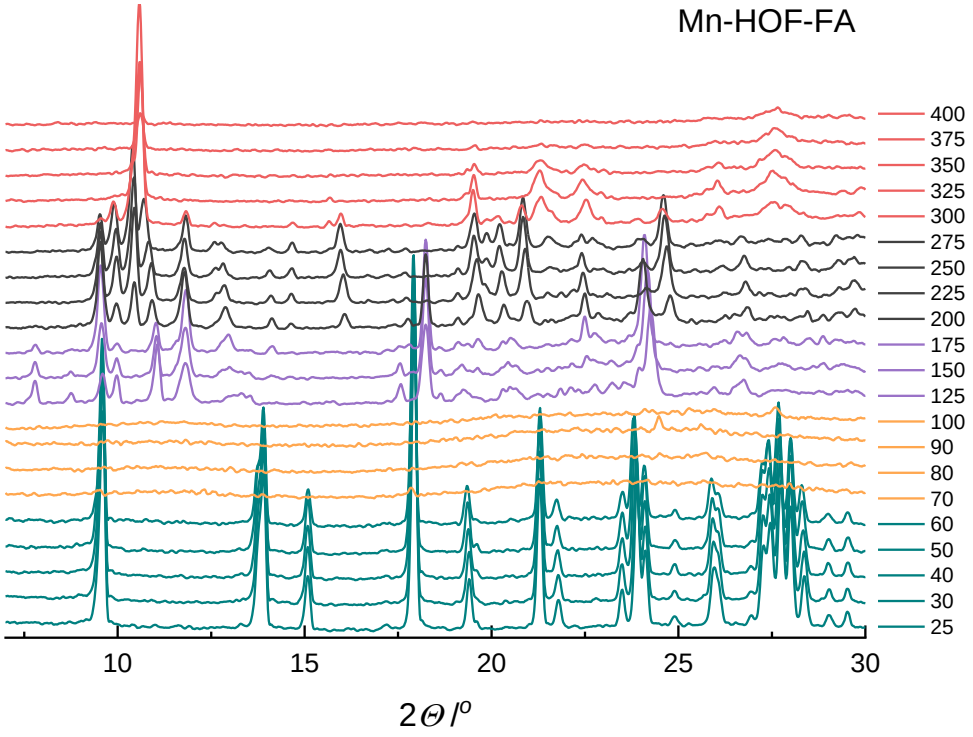

Figure S26. Temperature-dependent PXRD patterns for Mn-HOF-FA.

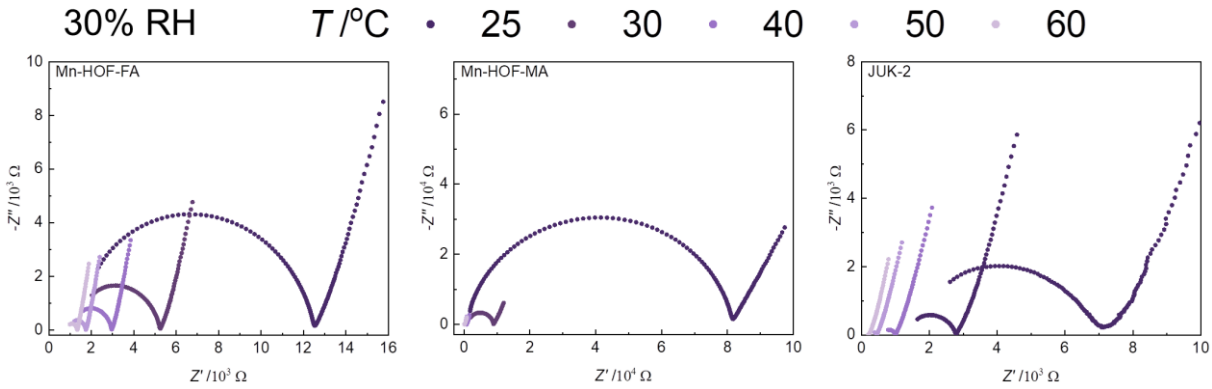

Figure S27. Variable temperature EIS conductivity measurements at 30% RH for Mn-HOF-FA (left), Mn-HOF-MA (centre) and JUK-2 (right).

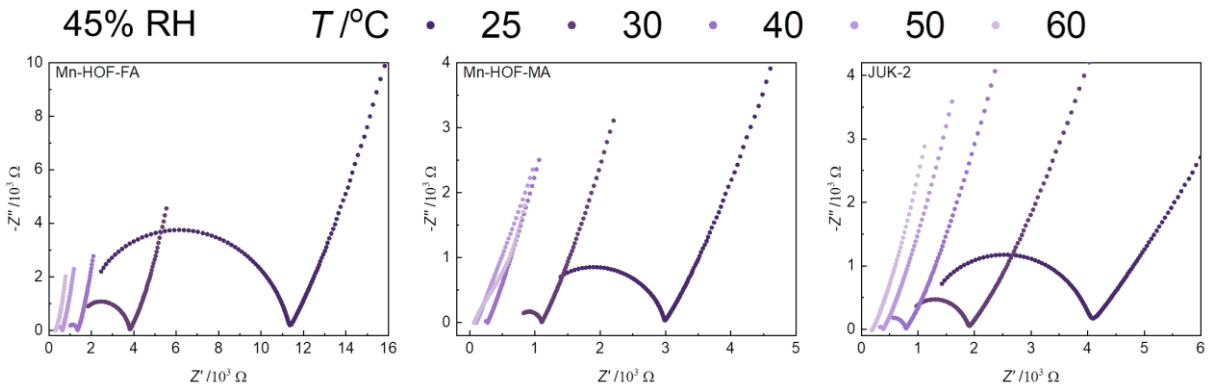

Figure S28. Variable temperature EIS conductivity measurements at 45% RH for Mn-HOF-FA (left), Mn-HOF-MA (centre) and JUK-2 (right).

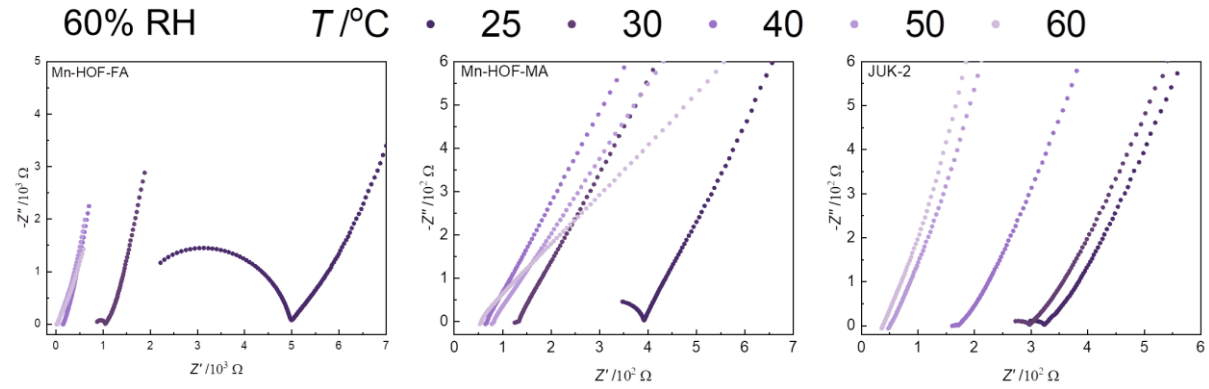

Figure S29. Variable temperature EIS conductivity measurements at 60% RH for Mn-HOF-FA (left), Mn-HOF-MA (centre) and JUK-2 (right).

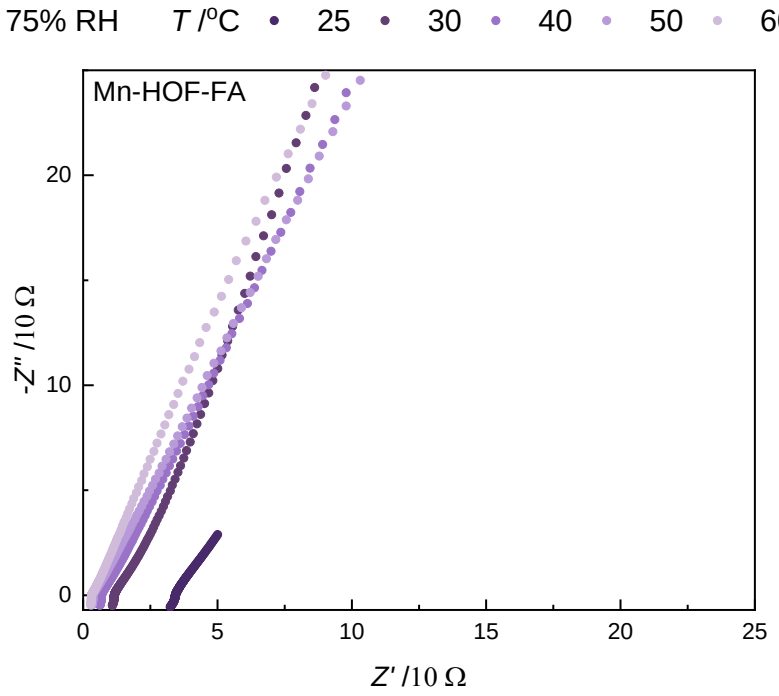

Figure S30. Variable temperature EIS conductivity measurements at 75% RH for Mn-HOF-FA.

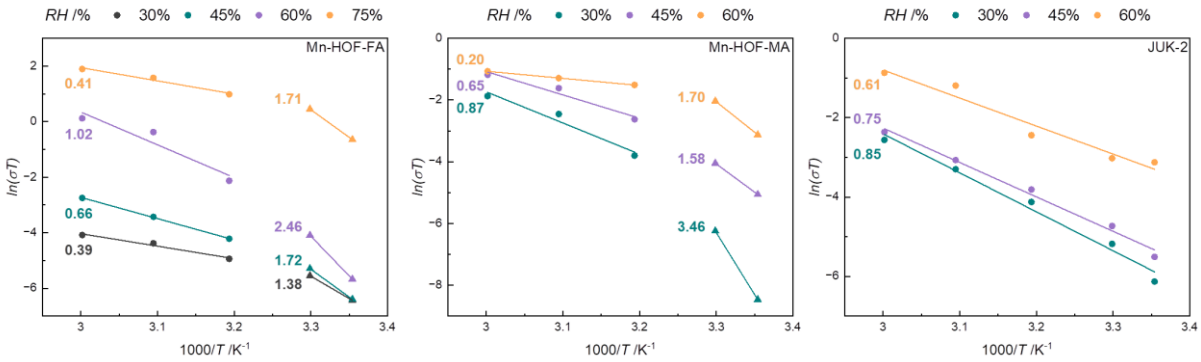

Figure S31. Arrhenius plots with activation energies indicated as numbers (in eV) at anhydrous conditions for Mn-HOF-FA (left), Mn-HOF-MA (centre) and JUK-2 (right).

Table S6. Comparison of proton conductivities for JUK-2 and Mn-HOFs.

RH (%)	Sample	Conductivity (S·cm^{-1})					Activation energy (eV)
		25°C	30°C	40°C	50°C	60°C	
30	Mn-HOF-FA	$5{,}4\times10^{-6}$	$1{,}3\times10^{-5}$	$2{,}3\times10^{-5}$	$3{,}9\times10^{-5}$	$5{,}1\times10^{-5}$	1,38; 0,39
	Mn-HOF-MA	$7{,}0\times10^{-7}$	$6{,}4\times10^{-6}$	$7{,}1\times10^{-5}$	$2{,}7\times10^{-4}$	$4{,}6\times10^{-4}$	3,46; 0,87
	JUK-2	$7{,}0\times10^{-6}$	$1{,}9\times10^{-5}$	$5{,}2\times10^{-5}$	$1{,}1\times10^{-4}$	$2{,}3\times10^{-4}$	0,85
45	Mn-HOF-FA	$6{,}0\times10^{-6}$	$1{,}7\times10^{-5}$	$4{,}7\times10^{-5}$	$1{,}0\times10^{-4}$	$1{,}9\times10^{-4}$	1,72; 0,66
	Mn-HOF-MA	$2{,}1\times10^{-5}$	$5{,}8\times10^{-5}$	$2{,}3\times10^{-4}$	$6{,}1\times10^{-4}$	$9{,}2\times10^{-4}$	1,58; 0,65
	JUK-2	$1{,}4\times10^{-5}$	$2{,}9\times10^{-5}$	$7{,}1\times10^{-5}$	$1{,}4\times10^{-4}$	$2{,}8\times10^{-4}$	0,75
60	Mn-HOF-FA	$1{,}0\times10^{-5}$	$6{,}0\times10^{-5}$	$3{,}8\times10^{-4}$	$2{,}1\times10^{-3}$	$3{,}4\times10^{-3}$	2,46; 1,02
	Mn-HOF-MA	$1{,}5\times10^{-4}$	$4{,}3\times10^{-4}$	$7{,}0\times10^{-4}$	$8{,}5\times10^{-4}$	$1{,}0\times10^{-3}$	1,70; 0,20
	JUK-2	$1{,}5\times10^{-4}$	$1{,}6\times10^{-4}$	$2{,}8\times10^{-4}$	$9{,}4\times10^{-4}$	$1{,}3\times10^{-3}$	0,61
75	Mn-HOF-FA	$1{,}8\times10^{-3}$	$5{,}2\times10^{-3}$	$8{,}5\times10^{-3}$	$1{,}5\times10^{-2}$	$2{,}0\times10^{-2}$	1,71; 0,41

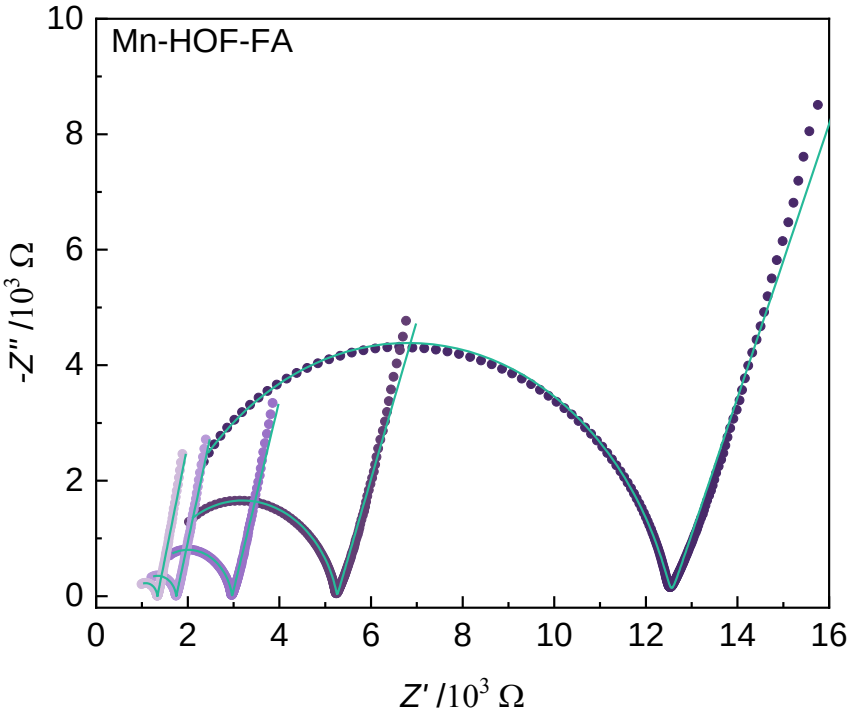

Figure S32. Representative temperature-dependent AC impedance plots at 30% RH for Mn-HOF-FA; purple circles – measured data, green line – fitted curves (with the use of ZSimpWin software).

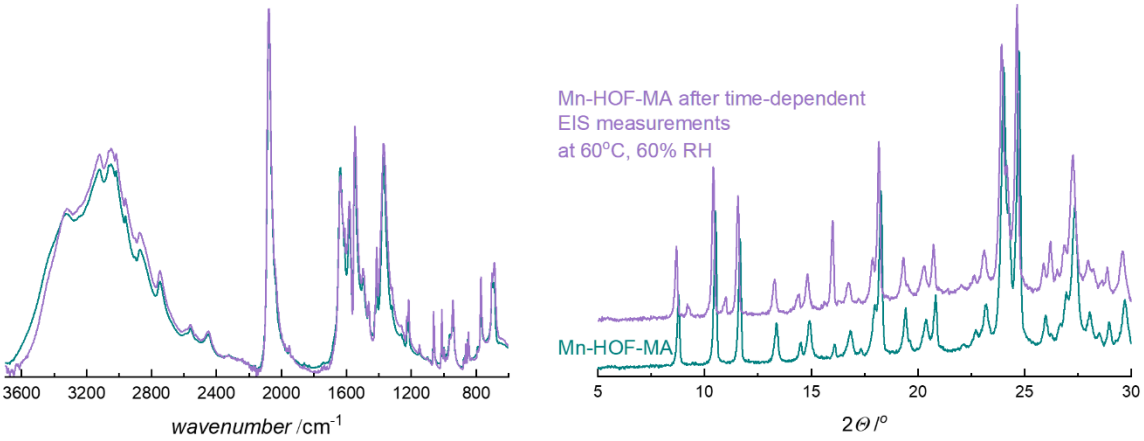

Figure S33. IR spectra (left) and PXRD patterns (right) of the as-synthesized Mn-HOF-MA (green) and after EIS measurement at 60°C at 60% RH (purple).

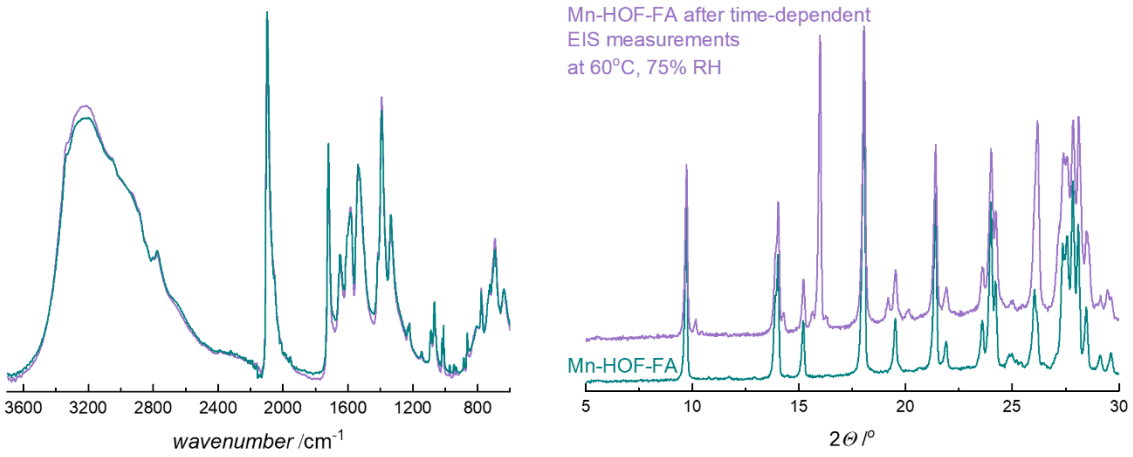

Figure S34. IR spectra (left) and PXRD patterns (right) of the as-synthesized Mn-HOF-FA (green) and after EIS measurement at 60°C at 60% RH (purple).

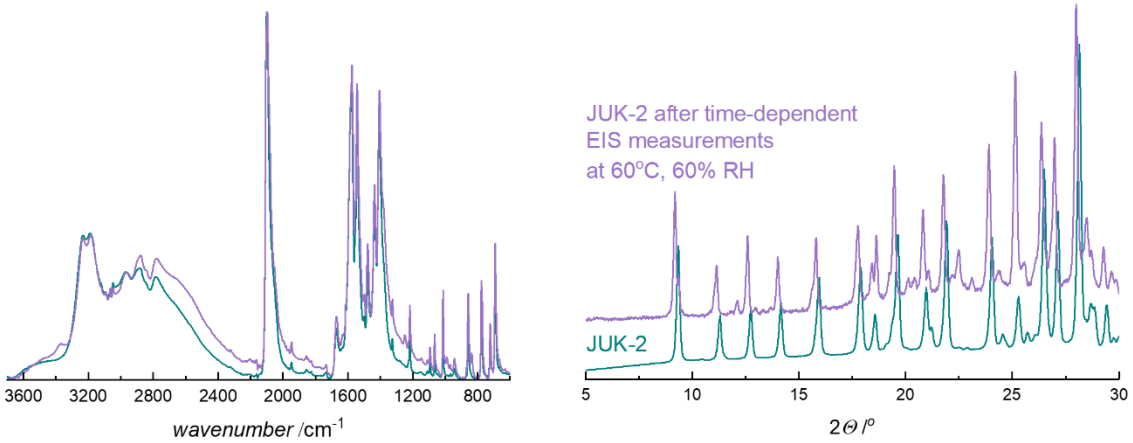

Figure S35. IR spectra (left) and PXRD patterns (right) of the as-synthesized JUK-2 (green) and after EIS measurement at 60°C at 75% RH (purple).

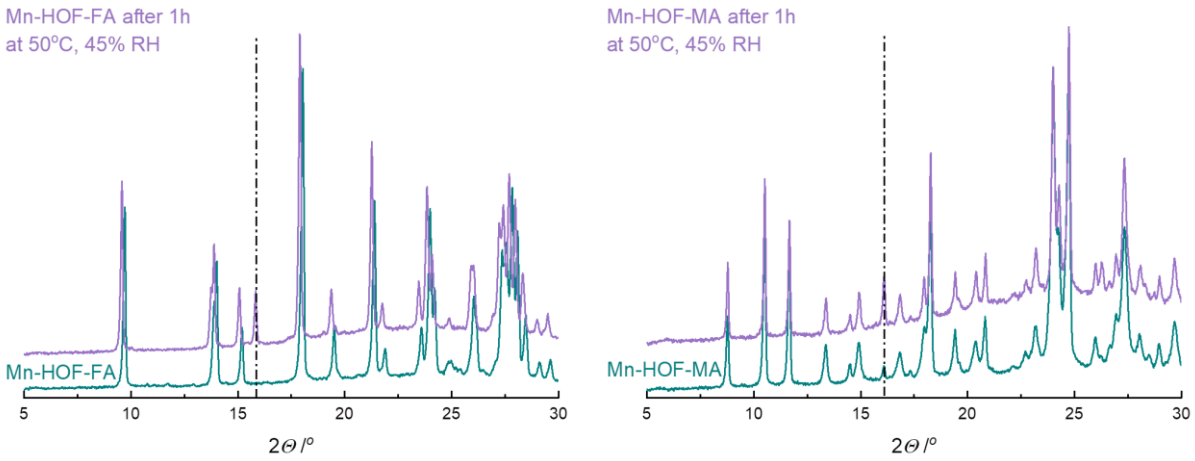

Figure S36. PXRD patterns of the as-synthesized Mn-HOFs (green) and after 1h at 50°C at 45% RH (purple).

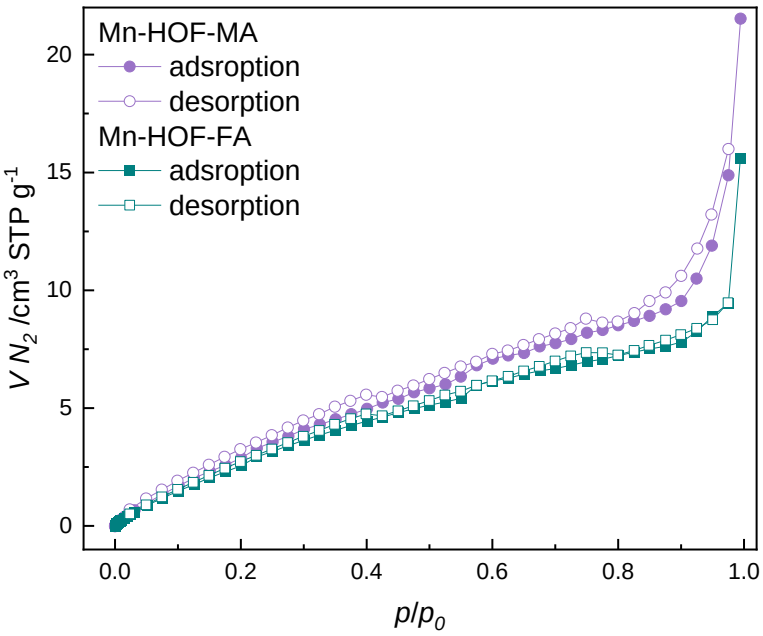

Figure S37. N_2 adsorption measurement at 77 K for Mn-HOF-MA (purple) and Mn-HOF-FA (green), closed symbols: adsorption, open symbols: desorption.

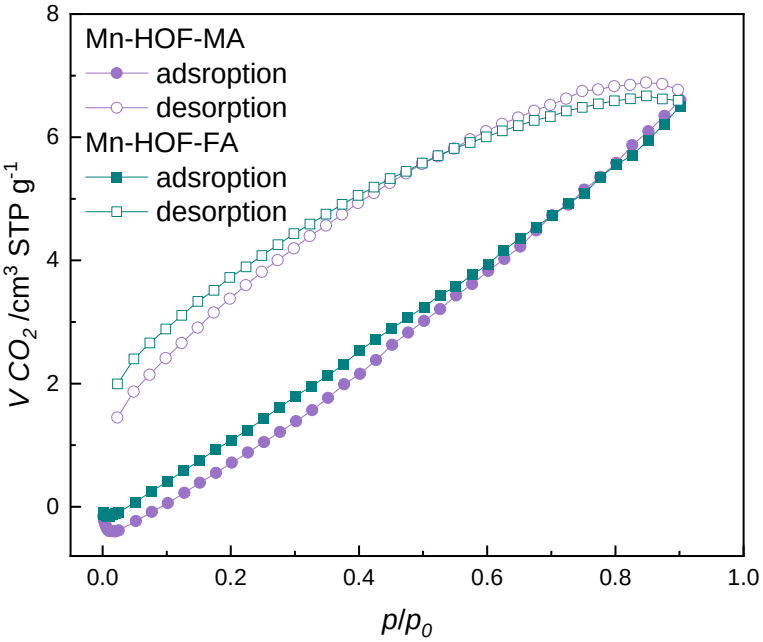

Figure S38. CO_2 adsorption measurement at 195 K for Mn-HOF-MA (purple) and Mn-HOF-FA (green), closed symbols: adsorption, open symbols: desorption.

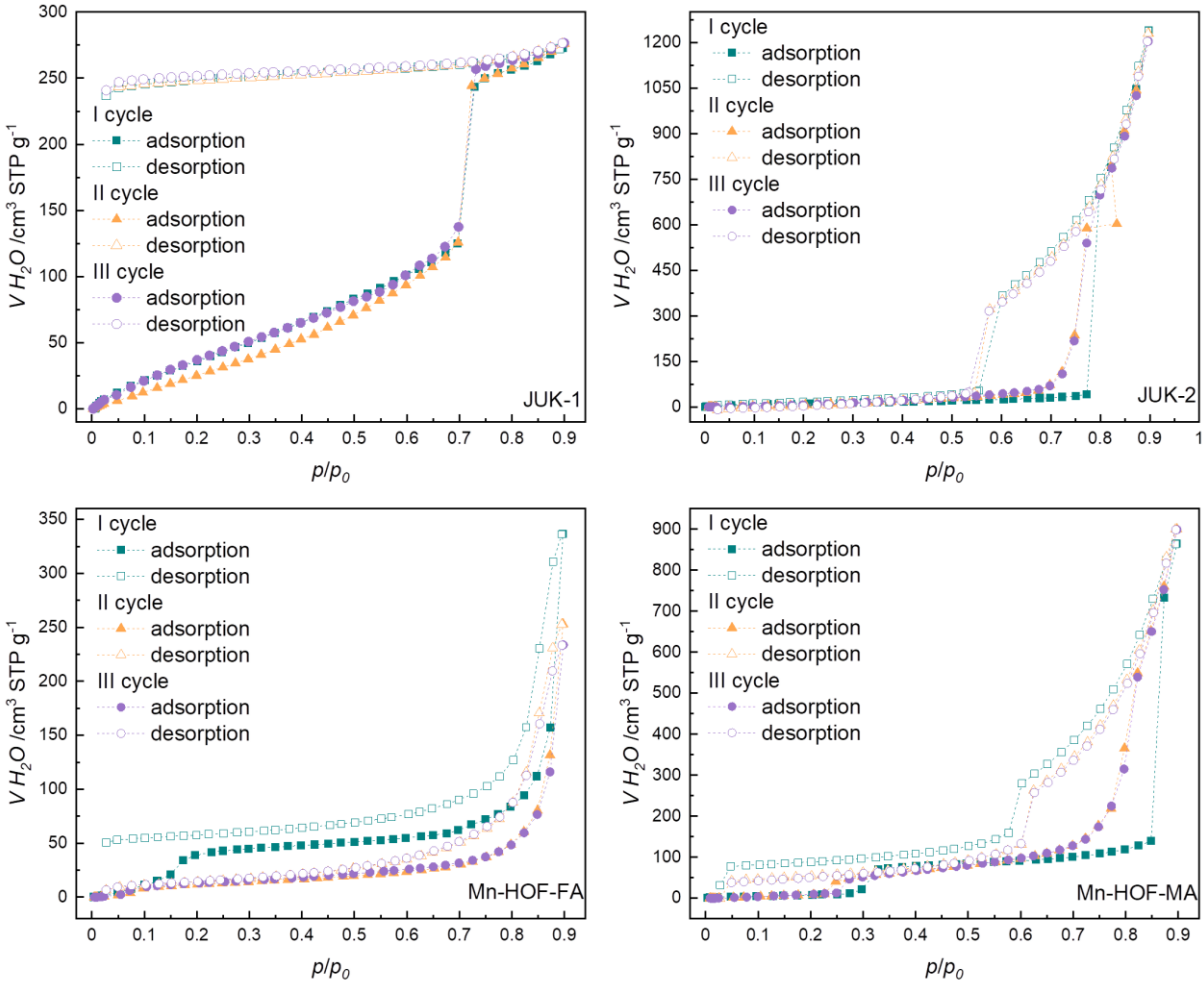

Figure S39. H_2O adsorption cycling test at 293 K for JUK-1, JUK-2, Mn-HOF-FA and Mn-HOF-MA, closed symbols: adsorption, open symbols: desorption.

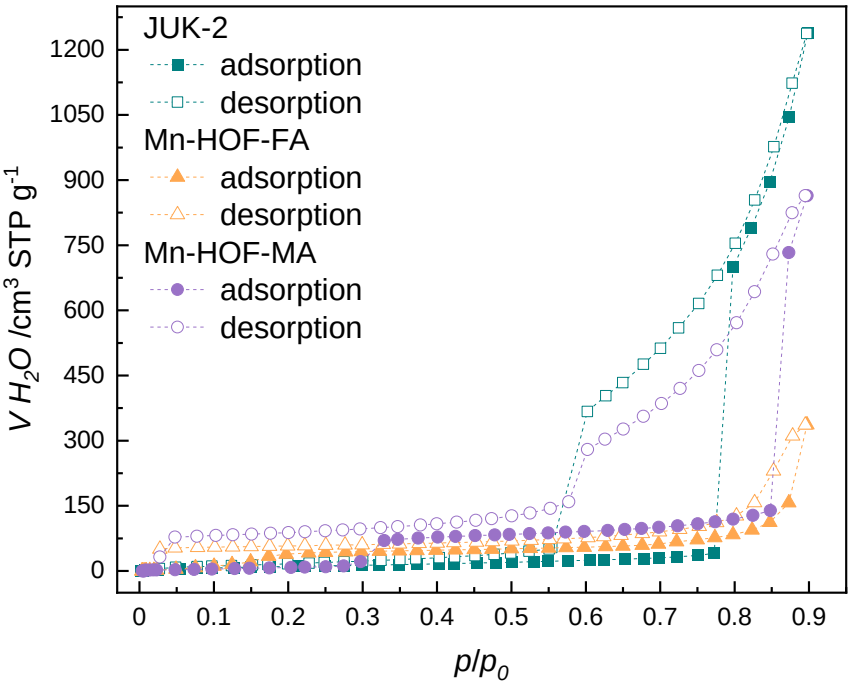

Figure S40. H_2O adsorption at 293 K for JUK-1, JUK-2, Mn-HOF-FA and Mn-HOF-MA, closed symbols: adsorption, open symbols: desorption.

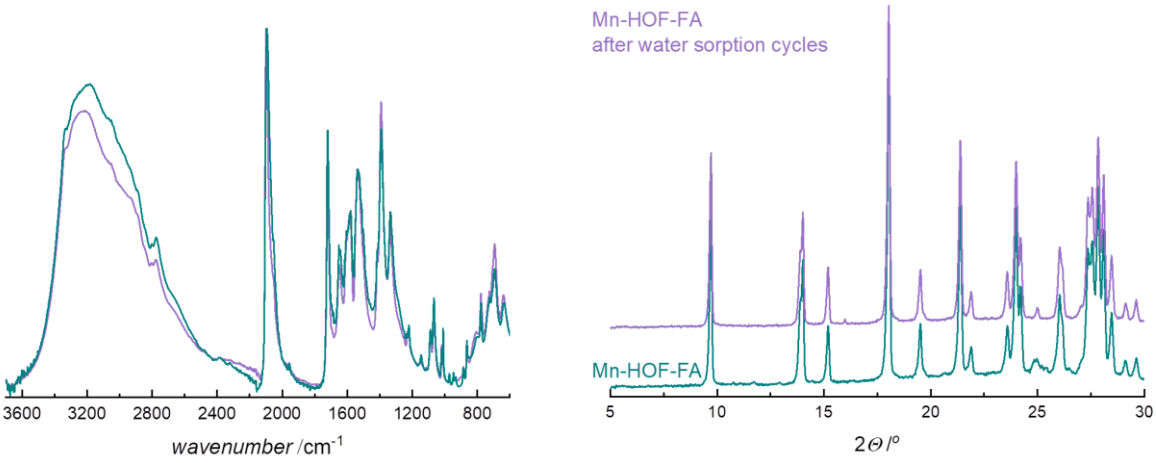

Figure S41. IR spectra (left) and PXRD patterns (right) of the as-synthesized Mn-HOF-FA (green) and after water sorption cycles (purple).

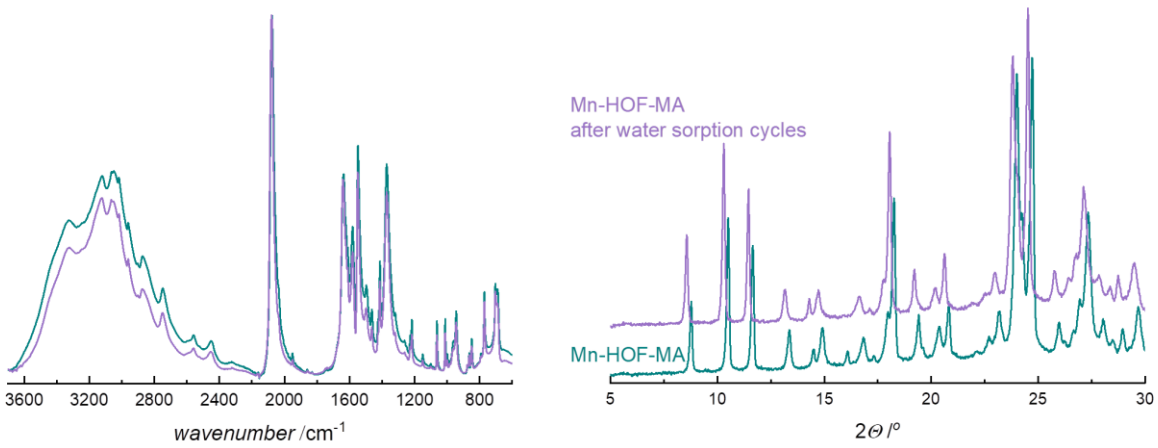

Figure S42. IR spectra (left) and PXRD patterns (right) of the as-synthesized Mn-HOF-MA (green) and after water sorption cycles (purple).

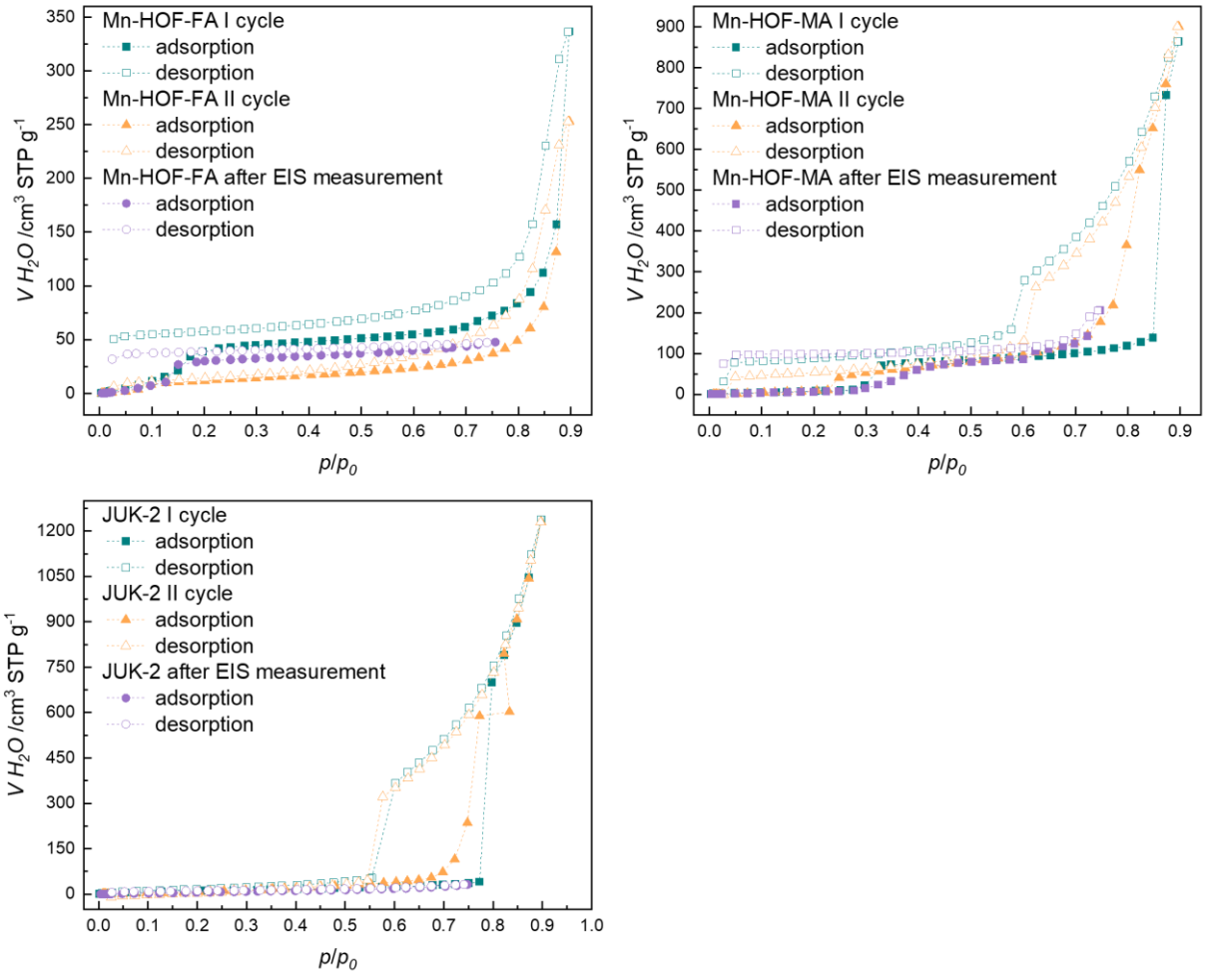

Figure S43. H_2O adsorption at 293 K for JUK-2, Mn-HOF-FA and Mn-HOF-MA after EIS measurement, closed symbols: adsorption, open symbols: desorption.

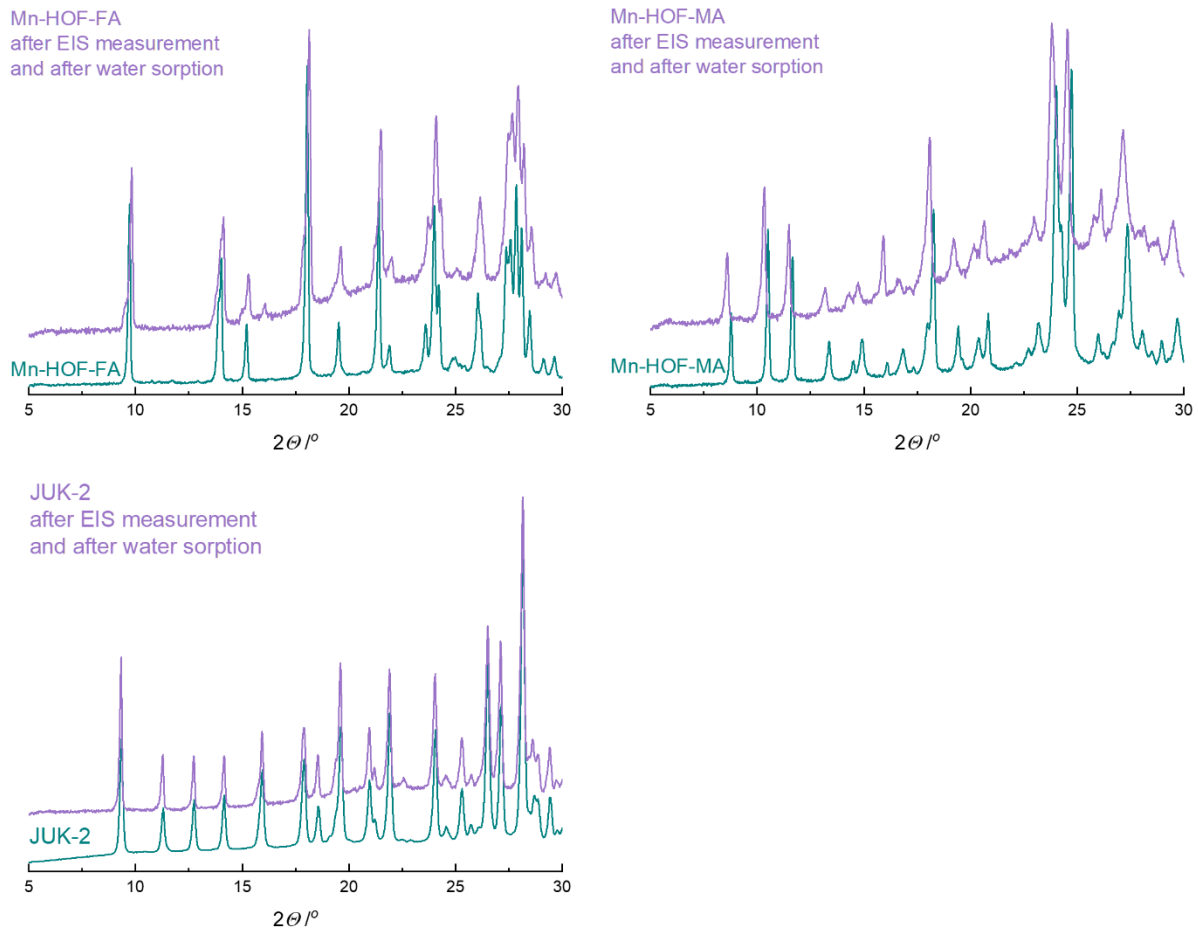

Figure S44. PXRD patterns of the as-synthesized JUK-2 and Mn-HOFs (green) and after EIS measurement and water sorption (purple).

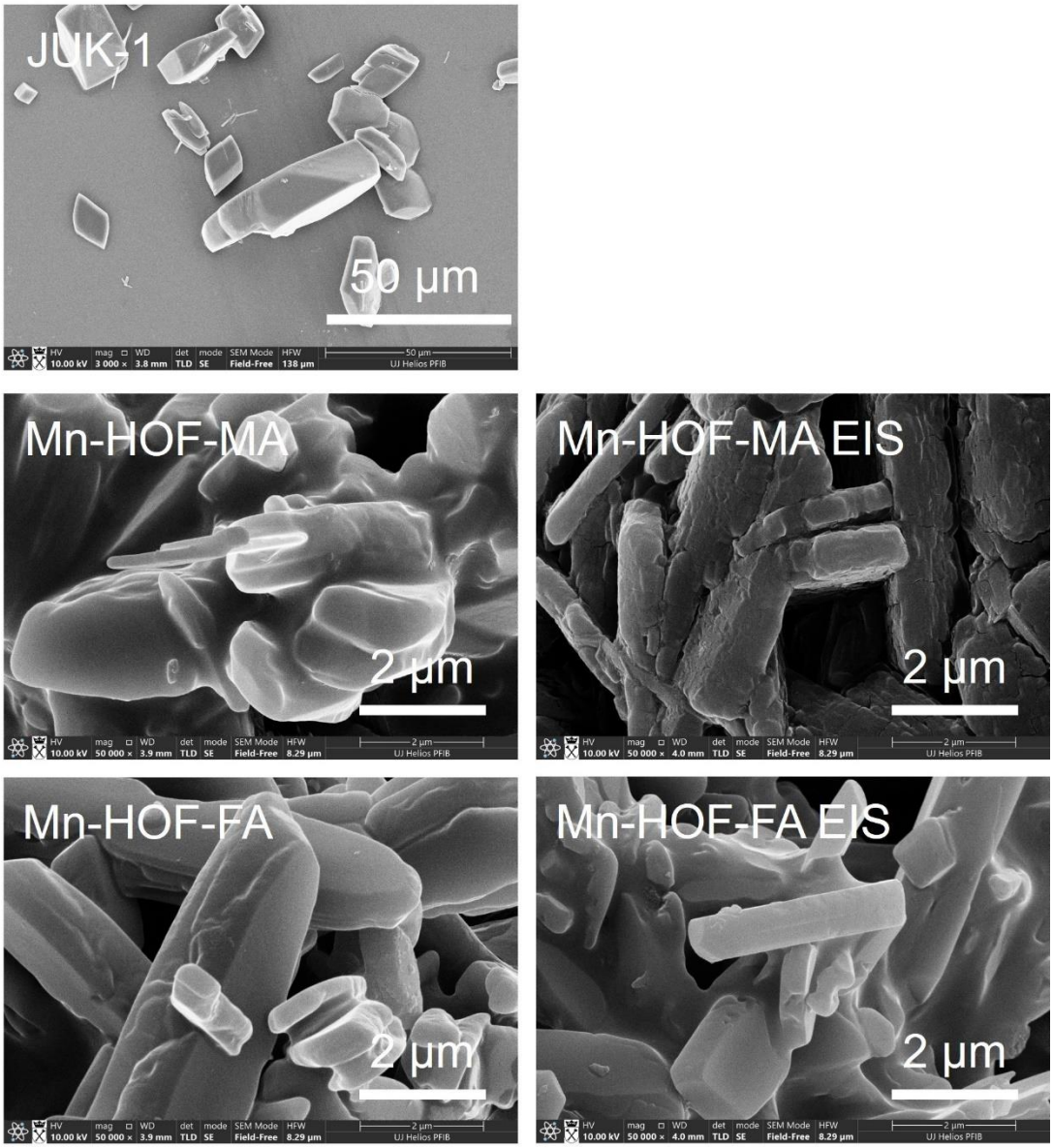

Figure S45. Scanning electron microscope (SEM) image of the as-synthesized JUK-1 and Mn-HOFs (left) and for Mn-HOFs after EIS measurement (right).

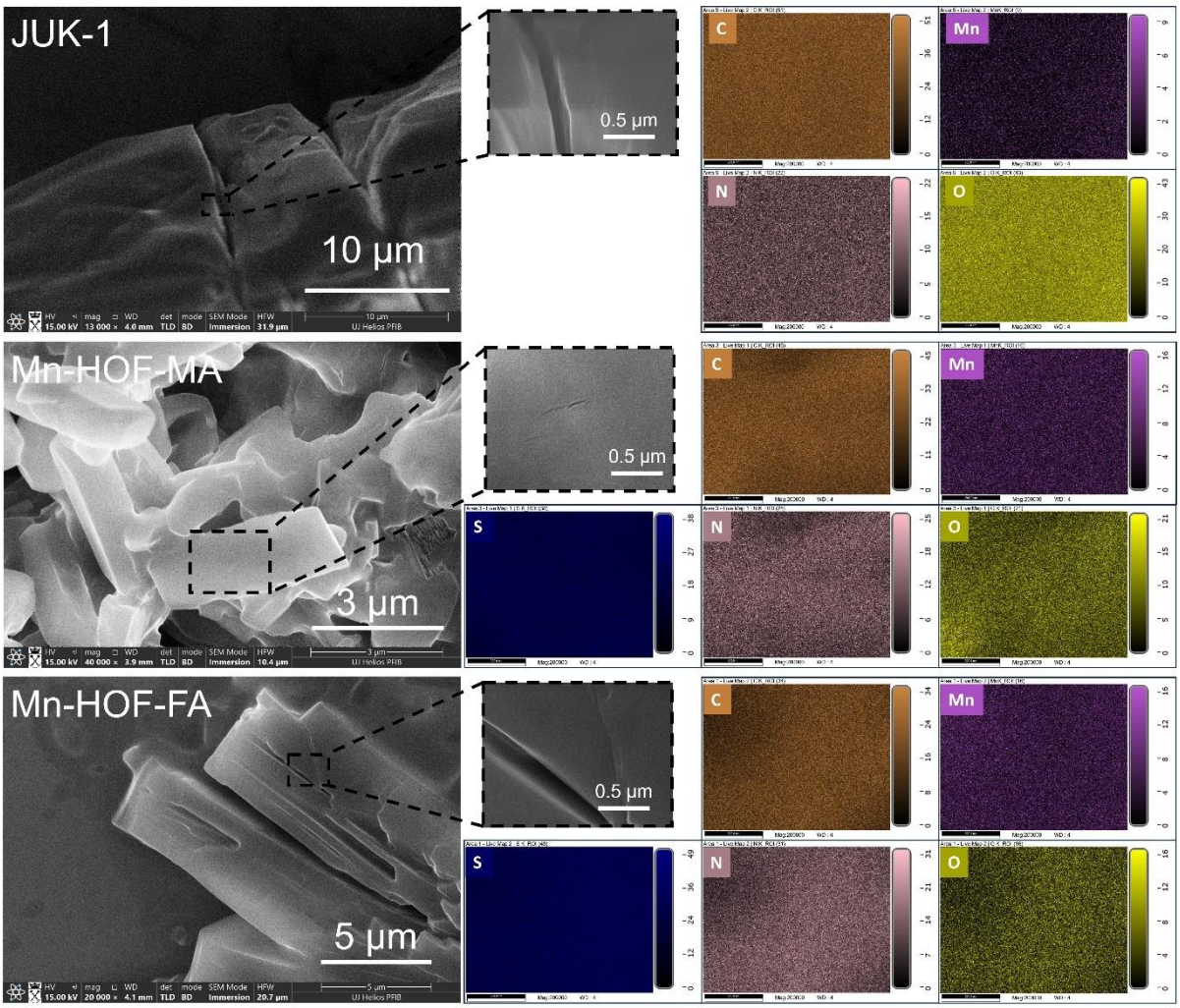

Figure S46. SEM image of the as-synthesized JUK-1 and Mn-HOFs and the elemental X-ray maps of manganese (purple), carbon (orange), oxygen (yellow), nitrogen (pink) and sulfur (blue).

References in the Supporting Information

1 D. Matoga, B. Gil, W. Nitek, A. D. Todd and C. W. Bielawski, *CrystEngComm*, 2014, **16**, 4959.

2 D. Matoga, M. Oszajca and M. Molenda, *Chem. Commun.*, 2015, **51**, 7637–7640.

3 A. Altomare, C. Cuocci, C. Giacovazzo, A. Moliterni, R. Rizzi, N. Corriero and A. Falcicchio, *J Appl Crystallogr*, 2013, **46**, 1231–1235.

4 V. Favre-Nicolin and R. Černý, *J Appl Crystallogr*, 2002, **35**, 734–743.

5 V. Petříček, L. Palatinus, J. Plášil and M. Dušek, *Zeitschrift für Kristallographie - Crystalline Materials*, 2023, **238**, 271–282.